Cutter Suction Spillage

On creating a numerical model for estimating spillage in a cutter suction dredger while cutting sand.

Alden Antony Louis

TU Delft

GREAT LAKES DREDGE & DOCK COMPANY RIVER & HARBOR IMPROVEMENTS

TECHNICAL UNIVERSITY OF DELFT

MASTER THESIS

Cutter Suction Spillage

Author:
Alden Antony Louis
S.N: 4455894

Thesis committee:
Prof. Dr. Ir. C. van Rhee
Dr. Ir. S. A. Miedema
Ir. B. J. Nieuwboer
Mr. R. C. Ramsdell
Dr. Ir. P. R. Wellens

A thesis submitted in fulfilment of the requirements for the degree of Master of Science

in

Offshore & Dredging Engineering
Specialization: Dredging

To be defended publicly Monday August 21, 2017 at 3:00pm

An electronic version of this thesis is available at https://repository.tudelft.nl/

August 9, 2017

Summary

This study was initiated by the need of the dredging industry to develop a working model that can accurately estimate spillage when using a cutter suction dredger for cutting soft material like sand. Spillage can be defined in many ways. Great Lakes defines spillage as "the difference in elevation between the maximum depth at which the dredge cuts (also known as cutting depth) and the depth obtained after dredging (also known as after dredging depth). Theoretically, spillage is defined as "the material that is displaced from the seabed which does not enter the suction pipe and thus does not contribute to production". The spillage percentage is defined as the ratio of spillage to the total cutting production (amount of material cut from the seabed). This means that the spillage percentage is a percentage of the total cutting production. Acquiring an accurate estimate of spillage can enable dredging companies to provide a more accurate production estimate thus reducing the risks involved in projects. The aim of this study is to identify and describe the types of spillage that occurs while dredging soft materials like sand and to use this information to create a numerical model that estimates spillage.

Four types of spillage are identified namely, type 1 spillage – soil that disintegrates and is directed away from the cutter head, type 2 spillage – soil that enters the cutter head but not the suction mouth, type 3 spillage – soil that does not enter the cutter head when the bank height is large relative to the cutter head (single pass) and lastly, type 4 spillage – breaching of the bank after the cutter head has passed. In this study, focus is given only to type 2 spillage.

The literature on spillage is limited and the major contribution comes from the work done by Burger (2003). Burger performed a series of experiments and developed simulation models to identify the spillage process. Experiments involving single particle behavior were performed and the residence time of particles were studied by varying the rotational velocity of the cutter head and the suction flow. Using the measured values of residence time, the filling degree of the cutter head was estimated but the values obtained were very high which implied that residence time for single particles did not apply when the cutter head was actually cutting.

A simulation model was also set up in order to describe the trajectories of the particles inside the cutter head. The flow inside the cutter head was subdivided into a flow as a result of rotation of the cutter head (forced vortex) and a flow due to suction (sink). A

force balance equation was used to obtain the equation of motion for a single particle with the forces being the gravitational force, drag force, pressure gradient force and added mass force. A qualitative explanation was given for the low production in the overcut situation when compared with the undercut situation as witnessed in the industry.

Actual cutting tests were also performed by Burger in order to determine production and spillage as a function of the operational parameters of the cutter head. The influence of the rotational velocity on the trajectories of particles were studied during under-cutting and over-cutting. Also, the influence of the ladder angle on production was studied. During the tests, the particle diameters were varied and it was observed that the production percentage reduced with increasing particle diameters.

In the seventies, extensive research was performed on flows near and within the cutter head. The main observation was that the cutter head behaved like a combination of an axial and centrifugal pump with an inflow near the nose of the cutter head and an outflow close to the cutter ring. The theory for the model is based on the fact that the cutter head behaves like a pump and the pump affinity laws are used as the base for the model.

The cutter head is divided into two slices with each slice behaving like a pump. Using the pump affinity laws, equations for the pressure and flow in the two slices are derived. The theory assumes that the outgoing flow close to the cutter ring circulates back into the cutter head as the ingoing flow near the nose. The most important parameter is the height of the bottom slice (w_1) since the other parameters are dependent on it. Thus, an implicit equation for w_1 is obtained and solved using an iterative process. Using w_1, the outgoing flow is calculated which is basically the circulating flow. Spillage is defined as the ratio of the circulating flow to the total outgoing flow. The input data of the model is directly taken from one of the dredges of GLDD, The Texas and a spillage of 38% is estimated.

A sensitivity analysis is performed using the operational parameters of the cutter head namely, rotational velocity, suction flow and the swing speed. Also, a sensitivity analysis is performed on β (constant influencing flow). It is observed that an increase in rotational velocity increases spillage whereas an increase in the suction flow decreases spillage. Compared with the rotational velocity and the suction flow, the swing speed did not have a large influence on spillage but an increase in swing speed did increase spillage.

Hydrographic surveys are used to calculate real-life spillage values. Contours representing the cutting production and the actual production obtained are drawn on these graphs and

the difference between the two yields the amount of spillage. Thus, spillage (%) is calculated as the ratio of the amount of spillage to the cutting production. Since during the project many issues were present, the spillage values are scattered ranging from 20% - 34%. When compared with the spillage estimated by the model (38%), it can be said that the model provides a value that is in close proximation with values observed in the industry. For further validation, results from the model are compared with the results obtained from the experiments performed by Burger (2003). The behaviour of the mixture velocity and that of the rotational velocity are found to be similar to what Burger observed in his experiments

Hence, it is concluded that although the current model is simple, the results obtained from it replicate what is witnessed in the industry and thus provides a good estimate of spillage. The model can definitely be improved upon and some of the recommendations include taking into account the internal volume of the cutter head as well as the cutter head geometry. Particle – particle interaction should be incorporated in the model along with particle shape/size. The flow field within the cutter head will play an important role and thus a CFD package needs to be used to obtain a better approximation of spillage.

Acknowledgements

First off, I would like to thank Prof. Dr. Ir. Cees van Rhee, the chairman of the committee, for trusting me with this challenging project. I would also like to express my sincere gratitude to my supervisor Dr. Ir. Sape Miedema for his guidance and continuous support. Moreover, I would like to thank my supervisor Mr. Robert C. Ramsdell from Great Lakes Dredge & Dock (GLDD) for the countless hours he set aside for me to discuss about my thesis and provide pointers in order to help me progress. Last but not the least, I would like to thank Ir. Bas Nieuwboer for his insightful comments offered during my MSc thesis.

Besides my advisors, I would like to thank the Production team at GLDD for walking me through the estimation procedure and providing me with real-life data from various projects in order to optimize my model. Special thanks need to be dispensed to Bradley McConnon who, despite his busy schedule, sat down and bounced ideas with me for the model. A very special thanks to my girlfriend, Richele, who supported me and gave me confidence during the entire duration of my thesis.

Finally, I would like to thank Femiwa, Sahil, Briggs and also my family for their immense support during my post-graduate studies at TU Delft.

Contents

List of Figures

List of Tables

List of Symbols

a	= Ratio of densities (slice 1/slice2)	-
b_2	= Breadth between shrouds at outlet of a pump	m
C	= Ratio of blades angles (slice 2/slice 1)	-
D_o	= Diameter at the cutter ring	m
D_i	= Diameter at the nose	m
D_m	= Diameter at the interface of 2 slices	m
D_1	= Average diameter in slice 1	m
D_2	= Average diameter in slice 2	m
f	= Factor	-
F_{cut}	= Cut face (depth of cut)	m
g	= Gravitational constant	m/s^2
H	= Head	m
n	= Rotational velocity of the cutter head	rps
p_1	= Pressure in slice 1	Pa
p_2	= Pressure in slice 2	Pa
q_1	= Specific flow (slice 1)	m^2/s
q_2	= Specific flow (slice 2)	m^2/s
Q_1	= Outgoing flow (slice 1)	m^3/s
Q_2	= Ingoing flow (slice 2)	m^3/s
Q_c	= Circulating flow	m^3/s
Q_m	= Mixture flow	m^3/s
Q_p	= Cutting production	m^3/s
Q_T	= Total outgoing flow	m^3/s
S	= Step size	m
v_{swing}	= Swing speed	m/s
w	= Height of the cutter head	m
w_1	= Height of slice 1	m

w_2	= Height of slice 2	m
α	= Constant	-
β	= Constant	-
ϕ_1	= Blade angle (slice 1)	degrees
ϕ_2	= Blade angle (slice 2)	degrees
ρ_1	= Density in slice 1	kg/m^3
ρ_2	= Density in slice 2	kg/m^3
θ	= Cutter head angle	degrees

1 Introduction

The aim of this study is to identify and describe the types of spillage that occurs while dredging soft materials like sand and to use this information to create a numerical model that estimates spillage. This study was initiated by the need of the dredging industry to develop a working model that can accurately estimate spillage when using a cutter suction dredge. Spillage can be defined in many ways. Great Lakes defines spillage as “the difference in elevation between the maximum depth at which the dredge cuts (also known as cutting depth) and the depth obtained after dredging (also known as after dredging depth). Theoretically, spillage is defined as “the material that is displaced from the seabed which does not enter the suction pipe and thus does not contribute to production”. The spillage percentage is defined as the ratio of spillage to the total cutting production (amount of material cut from the seabed). This means that the spillage percentage is a percentage of the total cutting production. Acquiring an accurate estimate of spillage can enable dredging companies to provide a more accurate production estimate thus reducing the risks involved in projects.

1.1 Cutter suction dredge

Cutter suction dredges are generally used for dredging shallow to medium waterways and harbours. Due to its ability to cut a wide variety of soil types and its precision, the cutter suction dredge is still widely used despite the trailing suction hopper dredge dominating the dredging market. Figure 1 shows an example of a cutter suction dredge.

Cutter suction dredges work in stationary mode either on spuds or anchors and have flexible discharge alternatives. They can either discharge into barges or through discharge pipelines to the placement site. By the use of booster pumps in the discharge lines, they can transport and place materials at considerable distances from the work site.

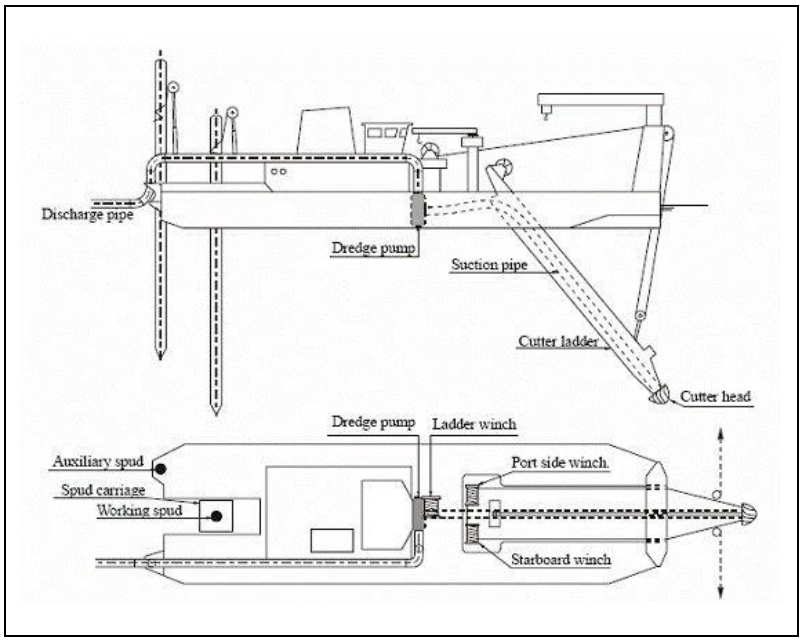

Figure 1: Cutter suction dredge and indication of components

The most integral component is the cutter head which is responsible for the actual excavation of soil. It excavates the soil into suitably sized material and is then sucked into the suction pipe in the form of solid/water slurry which is then pumped to the surface. A typical cutter has five or six blades. Figure 2 shows the cutter head of The Texas (GLDD). The cutter is attached to the ladder arm in front of the suction inlet. The ladder arm allows the cutter head to be raised and lowered to different depths. The maximum ladder angle (angle between the ladder and the horizontal) is about 45 degrees. Larger angles lead to high spillage which is generally undesirable.

A cutter head has 2 functions. One is to cut and dislodge the material from the sea bed and the second is to create a mixture of the cut materials and water to transport to the surface. The mixture is sucked in through the suction mouth placed at the lower half of the cutter head which is connected to a suction pipe that runs along the ladder arm back to the dredge.

Figure 2: Cutter head (screened) of The Texas (GLDD)

1.2 Working principle

As mentioned earlier, cutter suction dredges work in stationary mode. There are two types of cutter suction dredge: one that employs a spud carriage system wherein the work spud is placed in a carriage at the stern of the dredge and one that employs a fixed spud system wherein both the work spud and the auxiliary spud are in fixed positions located at the stern of the dredge.

Spuds are large anchor piles that are driven into the ground to keep the dredge stationary and advance the dredge forward when required. The dredge swings about the spud pole by means of side winches that are fastened by cables to side anchors. By slackening one anchor cable and pulling the other anchor cable, the dredge makes a circular motion about the spud pole.

In a spud carriage system, the spud pole, about which the dredge swings, is the work spud and is located on the spud carriage. Figure 3 shows the layout of a spud carriage system. When the work spud is fixed to the bottom, the dredge can move forward by pressing the cylinder to the stern. When the cylinder has reached the end of its stroke the second spud pole, the auxiliary spud, is lowered and the working spud is raised. The spud carriage is moved towards its initial position, the work spud is lowered and the auxiliary spud is raised again.

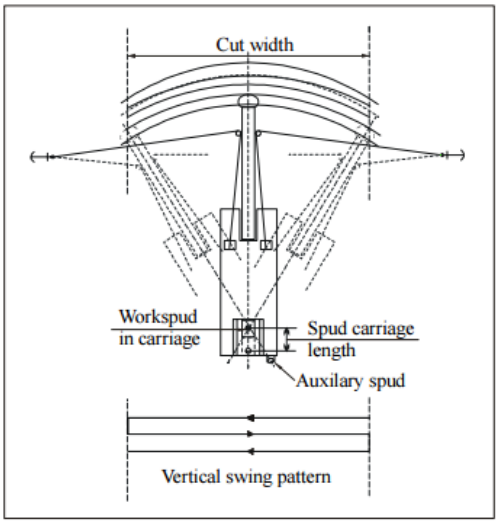

Figure 3: Spud system and swing pattern of a CSD

The cut face (depth of cut) is defined as the amount of material that is cut per swing of the dredge. After one complete swing, the dredge moves forward and starts the next swing. This distance that the dredge moves forward is called the step. The speed with which the dredge swings is called the swing speed.

The direction in which the cutter head rotates is always constant and is determined by the orientation of the teeth. Depending on the direction of swing, cutting can be of two types: under-cutting and over-cutting. In the under-cutting scenario, the blades move in the same direction as that of the swing and thus the teeth start cutting from the bottom of the bank. The blades push the cut material away from the suction mouth and there is a tendency for the particles to be thrown out of the cutter. In the over-cutting scenario, the blades move in the opposite direction as that of the swing and thus the teeth dig into the top of the bank. Here the blades bring the material towards the suction mouth.

1.3 Scope and outline of thesis

As stated in the earlier section, spillage is defined as the amount of material that is displaced from the seabed which does not enter the suction pipe. The factors that contribute to spillage could be the cutting process, mixture forming process within the cutter head, soil properties, cutter head geometry and operational parameters. The classification of spillage is as follows:

- Soil that disintegrates and is directed away from the cutter head. (Type 1).
- Soil that enters the cutter head but not the suction mouth (Type 2).
- Soil that does not enter the cutter head when the bank height is large, relative to the cutter head – single pass (Type 3).
- Breaching of the bank after the cutter head has passed (Type 4).

The types of spillage will be explained in greater detail in the upcoming chapter. In this study, we will only focus on the type 2 spillage.

2

Spillage

The types of spillage are defined previously so in this chapter each type will be explained in detail including the factors that affect them.

2.1 Type 1 spillage

Soil that disintegrates and is directed away from the cutter head.

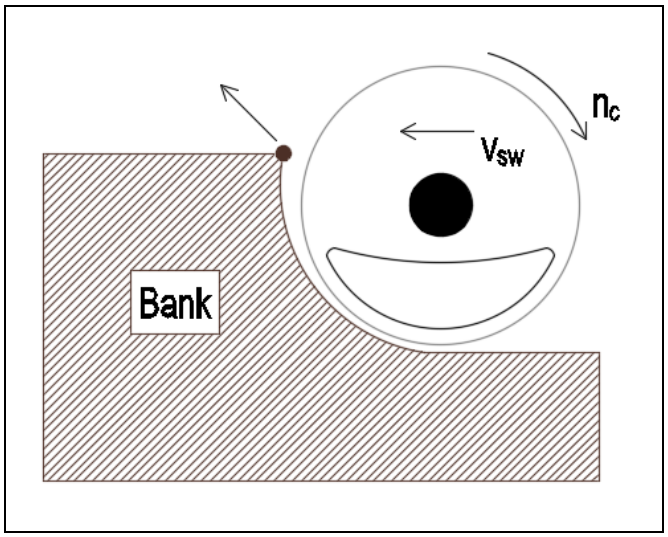

Figure 4: Breaking of particles while under-cutting.

This type of spillage generally occurs when cutting large particles such as rock, cemented material or gravel/cobbles. It can occur in both under-cutting and over-cutting situations.

When the blades of the cutter head pierce into the seabed, the soil disintegrates at the edge of the cut face and is directed away from the cutter head. Due to this, the disintegrated soil is unable to enter the cutter head and is thus considered as spillage. The reason for this spillage type could be because of increased rotational velocity of the cutter head. An increase in the rotational velocity will increase the intensity of the cutting process thus agitating the soil and disintegrating it.

Quantifying this spillage type is rather difficult because predicting the trajectories of the disintegrated soil is not easy. Also, if the disintegrated soil falls in the swing path of the cutter head then it has the opportunity to enter the cutter head again. Increasing the swing speed of the cutter head can cause a bull-dozing effect at the cutter head thus pushing the soil instead of cutting it. The best solution to reduce spillage is to find an optimum swing speed and rotational speed at which a desirable production can be obtained.

This spillage type can also be seen when cutting sand. In this case, the particles do not break off but are suspended into the water column. Once suspended they either settle back on the seabed or continue to move up to the water surface thus creating a plume. This spillage type is one of the reasons that contribute to the creation of this plume. Figure 5 shows the image of a plume formed due to a combination of various spillage types. In the event that the particles settle on the seabed instead of floating up to the water surface, these particles cannot be considered as spillage because there is a possibility that the cutter head could pick up these particles again.

Figure 5: Plume created while cutting sand using a CSD

2.2 Type 2 spillage

Soil that enters the cutter head but not the suction mouth.

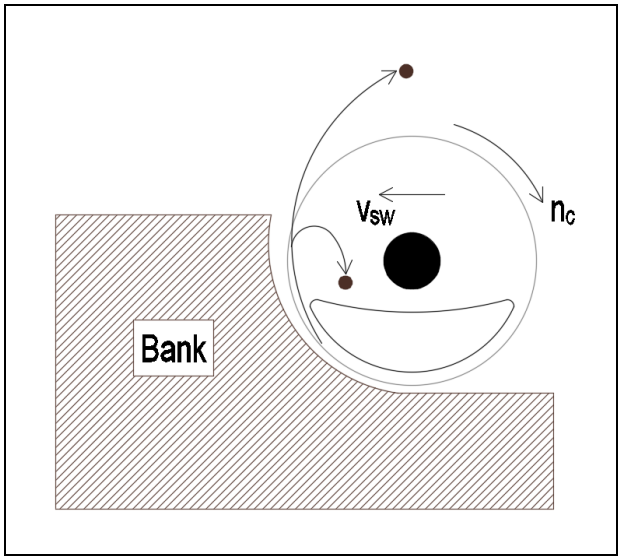

(a)

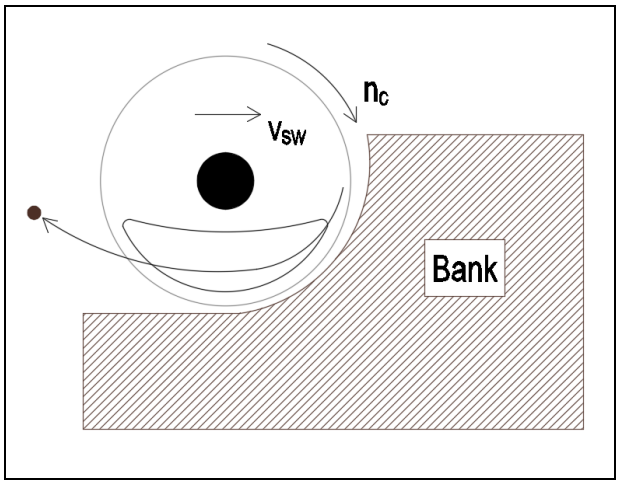

(b)

Figure 6: Trajectories of particles while undercutting (a) and over-cutting (b).

This type of spillage occurs differently in the under-cut and over-cut scenario. When the cutter head rotates, the blades cut the soil. In the under-cutting scenario, the soil is scooped up from the bottom of the bank. Here, the soil particles initially move in the same direction as the suction mouth but gravity works in the opposite direction and due to this, the particles will remain in the region of influence of the suction mouth for a longer duration thus giving the suction mouth an ample time to redirect the flow of the particles towards it. The main factor responsible is the rotational velocity of the cutter head. At low rotational velocities, the centrifugal forces acting on the particles are low and gravity acts as the dominating force. Due to this, the particles roll over the blades and settle at the bottom of the cutter head and escape through the gap in between the blades. Whereas at high rotational velocities, the centrifugal forces are dominant and due to this, the particles are thrown out of the cutter head.

In the over-cutting scenario, the blades dig into the top of the bank. Here, the soil particles move in a direction opposite to that of the suction mouth but gravity works in the same direction as that of the particles. Due to this, the particles achieve a higher velocity and quickly flow past the suction mouth thus being in its region of influence only for a limited duration of time.

The important parameters that affect this spillage type are the rotational speed of the cutter head, swing speed, ladder angle and mixture velocity of the suction mouth. An increase in the suction flow rate can counteract this spillage type bearing in mind that an optimum rotational velocity is taken into account.

2.3 Type 3 spillage

Soil that does not enter the cutter head when the bank height is large relative to the cutter head (single pass).

This spillage type usually deals with a large bank height. Figure 7 shows the diagram of a cutter head dredging a bank with a large bank height. The diagram shows that the bank height is a bit greater than the effective cutter head height and therefore only a single pass is required. Here the bank height is equal to the depth of cut. A single pass implies one swing of the cutter head along the width of cut in a single step whereas a multi-pass implies several swings along the width of cut in a single step. In a multi-pass, the sum of the depth of cut for each pass equals the total depth of cut. In the event that the depth of cut is larger than the effective cutter head height by a factor of 2-3, then multi-pass is usually employed.

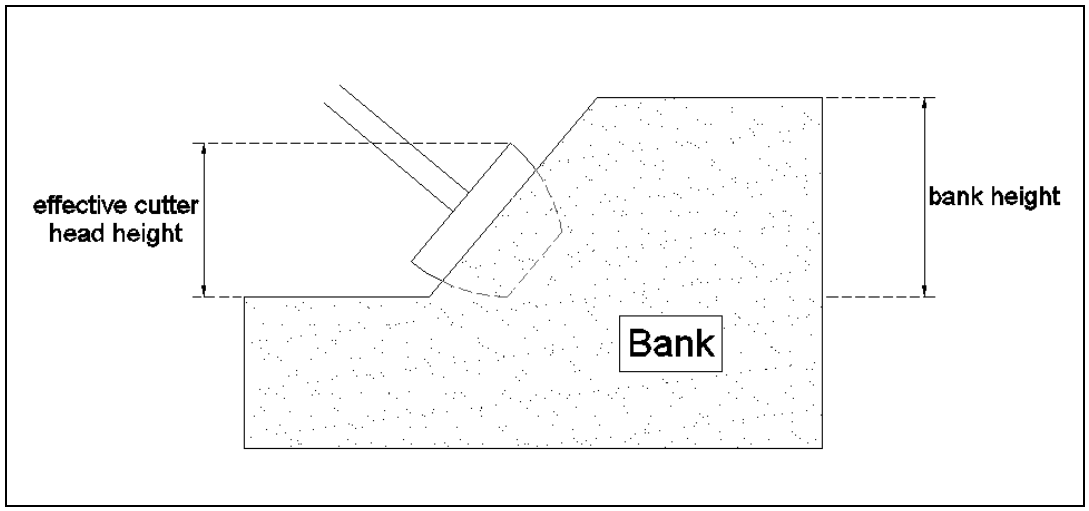

Figure 7: Diagram of a cutter head dredging a bank with a large bank height.

Figure 8 shows the steps involved in this type of spillage. In Figure 8(a), the cutter head is cutting a bank with a height greater than the effective cutter head. Thus, the part of the bank above the cutter head (cross-hatched) will fail since the cutter head is only able to cut the bank up to the cutter head height as shown in Figure 8(b). The failure of this bank causes the particles to fall on top of the cutter head and tries to force their way into the cutter head.

In essence, this process will definitely increase production as more particles enter the cutter head but once the filling degree of the cutter head becomes close to 100%, no more particles can enter the cutter head and thus the excess particles end up being spillage as evident in Figure 8(c). If high values of production are achieved when compared with spillage then this spillage type is not considered as a major concern. This spillage type is caused due to increased swing speed and increased cut face (bank height).

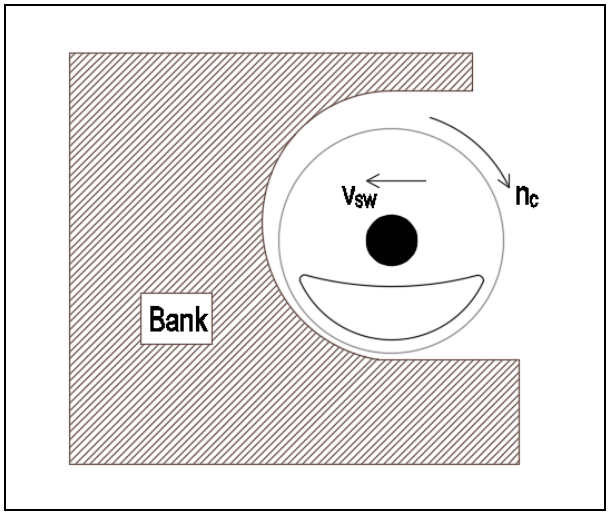

(a)

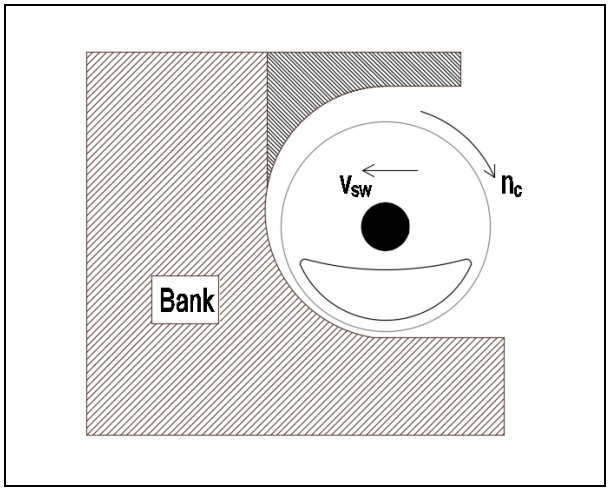

(b)

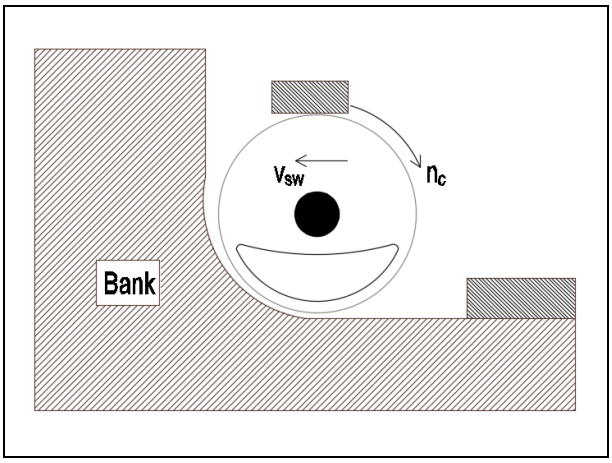

(c)

Figure 8: Steps involved when cutting a bank with a height greater than the cutter head

2.4 Type 4 spillage

Breaching of the bank after the cutter head has passed.

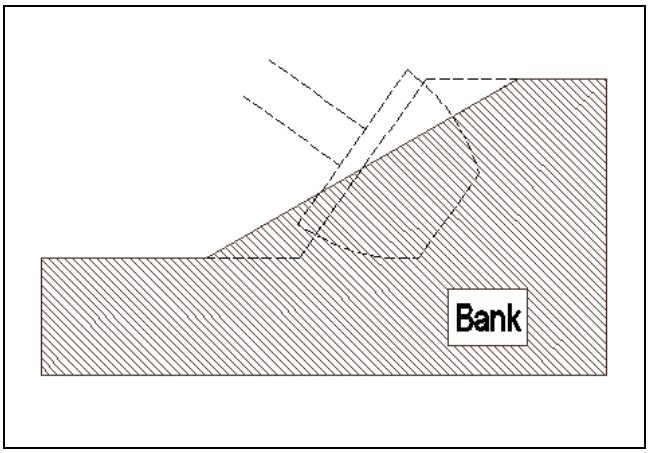

Figure 9: Breaching of the dredged bank.

This spillage type is usually seen in soft soil like sand and is generally associated with the wall velocity of the bank. The wall velocity can be seen as the propagation speed of a vertical disturbance on the bank. The slopes created after the cutter head passes can be steep due to the shear dilatancy effect of compacted sand (van Rhee, 1998). Dilatancy is the effect that the pore volumes of dense sand tend to increase during shear deformation as a result from increased shear stresses. When the sand is saturated with

water, it will lead to water under-pressure in the pores. Thus, the effective pressure is increased and also the shear resistance.

As this spillage type is generally witnessed in sand, it means that this generally occurs in soil that has high permeability. The initial slope formed after the cutter head has passed will not be stable in the long term. The sand will collapse off the bank, flow down the slope and settle at the foot of the slope as shown in Figure 9. The dotted slope indicates the initial bank developed. After the cutter head completes one swing, it will take a step and start the next swing. Due to this step, the cutter head will not pick up the soil deposited at the foot of the slope and thus, the deposited soil will be considered as spillage. In the event of a multi-pass, the swing speed of the cutter head will be modified in such a way that it matches with the failure rate of the bank thus reducing this type of spillage.

The amount of spillage is determined by the failure rate of the slope, swing speed of cutter head, width of the cut and bank height. If the swing speed of the cutter head is low then the bank has ample time to fail as the cutter will take more time to return to the same position during its next swing.

Also, if the width of the cut is too large once again the bank will have ample time to fail since the cutter will take more time to return to the same position during its next swing. This also occurs in side-slopes so spillage might be higher at the toe of the cut.

2.5 Summary.

Spillage is defined as the amount of material that is displaced from the seabed which does not enter the suction pipe. The different types of spillage are studied and the relevant parameters that cause these spillage types are identified with the primary parameters being the rotational velocity and the swing speed of the cutter. The current study focuses only on Type 2 spillage, i.e. soil that enters the cutter head but not the suction mouth.

3

Literature Review

3.1 Literature on mixture forming processes inside the cutter head.

Burger (2003) performed experiments at the laboratory of Dredging Technology at the Delft University of Technology, which focused on the behaviour of a single particle inside a cutter head. The aim behind these experiments was to better understand particle behaviour and their trajectories inside the cutter head. The production was determined by varying two velocities closely associated with a cutter head, the rotational velocity of the cutter and the suction flow inside the cutter. In the tests, the cutter head was placed in a concrete bank in a flume filled with water and the cutter head was not hauled. The haul velocity (swing speed) was neglected as it was an order of magnitude lower than the rotational velocity of the cutter head and the mixture velocity and thus would not have a significant influence on the behavior of particles within the cutter head. The cutter head was placed close to the bank and on both sides of the bank, holes were made through which particles were injected. The particles were injected into the cutter head through a tube that was connected with the holes. A jet of water was necessary to push the particles in between the blades and into the cutter head. This jet of water caused a disturbance in the flow inside the cutter but the velocity within the tube was of a lower magnitude than the suction flow and hence was ignored.

Initially the main focus was on measuring particle production but the data obtained were not accurate since particles that were thrown out of the cutter head were eventually sucked again resulting in 100% production. Although particles were sucked again, the duration it took to be sucked differed and so the residence time of the particles injected were noted. The residence time is defined as the time from the moment the particle is injected into the cutter until the particle is sucked up by the suction mouth.

The observations from the experiments were as follows:

- An increase in the mixture velocity generally saw a decrease in the average residence time of the particles.
- A general trend in the influence of the rotational speed on the residence time of particles was not found.
- A threshold value was observed for the rotational velocity of the cutter head. Below this threshold value, none of the particles were sucked up and the particles simply rolled over the blades. Above this threshold value, particles were taken up by the flow due to turbulence, collisions with the blades or lift and were sucked up.
- Finally, a decrease in the particle density showed a decrease in the residence times of particles.

An important parameter, called the filling degree of the cutter head, was introduced which indicated to what extent particle – particle interactions played a role and also how the flow was disturbed due to the presence of particles. The filling degree of the cutter head was estimated by using the measured values of residence time. The filling degree was defined as the ratio between the total volume of material inside the cutter head and the internal volume of the cutter head. Burger found that the total amount of material in the cutter head was about 85% of the volume of the cutter head, which was an unrealistically high value implying that the measured residence time for single particles did not apply when the cutter head was actually cutting as the haul velocity and particle - particle interactions could decrease the average residence time of a particle.

The residence time could be a major contributor to spillage. The probability of particles with high residence time to exit the cutter head is high since it has ample time to be influenced by the outgoing flow. Also, a decrease in residence time ideally means that particles are quickly sucked into the suction mouth and increasing the mixture velocity does increase production thus it is true that an increase in mixture velocity does decrease the residence time.

Burger (2003) also set up a simulation model in order to describe the trajectories of the particles inside the cutter head. The aim of the simulations was to obtain a better understanding of the processes taking place within the cutter head and so the influence of the flow inside the cutter head and the particle-flow interactions were investigated while particle-particle interactions were neglected.

The flow inside the cutter head was subdivided into a flow as a result of the rotation of the cutter head and a flow due to suction. The flow due to the rotation of the cutter head was represented by a forced vortex neglecting turbulence. Burger used the force balance equation in order to obtain the equation of motion for a single particle. The forces considered were: gravitational force, drag force, forces due to pressure gradients and added mass force. The flow inside the cutter head was represented by the superposition of a forced vortex and a sink.

An extended series of simulations was performed by varying the values of the operational parameters and the initial position of the particles and was concluded that only particles close to the suction mouth were sucked up. Also, with regard to production, an increase in rotational velocity always had a negative influence. It was observed that increasing the density of particles resulted in larger centrifugal acceleration of the particles and thus particles were thrown out of the cutter head faster. This was generally observed at higher rotational velocities of the cutter head. One of the limitations observed during the simulations performed was the absence of the pump effect of the cutter head in the flow model which could be crucial to determine particle trajectories.

Simulations representing the under-cut and over-cut simulation gave a qualitative explanation for the low production in over-cut situation as seen in the industry. This was due to the fact that as a particle was cut in the over-cut situation, water velocities and gravitational force were in the same direction over a large part of the particle trajectory. Hence the particle was continuously accelerated and had a high velocity as it passed the suction mouth. Moreover, the suction mouth moved in the opposite direction of the particle, meaning that the particle was in the area of influence of the suction flow for a very short duration. The suction flow was not strong enough to deflect the particle towards the suction mouth in such a short period of time.

Meanwhile, in the under-cut situation the particle velocity was lower because the water velocities and gravitational force were in the opposite direction and the particle

initially moved in the same direction as that of the suction mouth. Therefore, the suction flow had a stronger influence on the particle over a longer period of time.

Using the force balance equation by considering the forces acting on a single particle seemed promising. If the forces mentioned above were considered then a suitable equation could have been developed which could have been solved using a CFD package but since this thesis aims to achieve a simple model using excel, this approach wasn't taken into account.

In order to determine the influence of concentration of particles inside the cutter head, Burger (2003) performed actual cutting tests on a model scale. This made it possible to determine production and spillage as a function of the operational parameters of the cutter head (rotational velocity and suction flow). The artificial bank was made of weakly cemented gravel. A transparent back plate was used in the experiments in order to compare the particle trajectories from the cutting tests with the simulated particle trajectories discussed earlier. The aim was to focus on the mixture processes that took place inside the cutter head. Some of the results of the experiment were:

- In under-cutting, it was observed that an initial increase in rotational velocity resulted in an increase in production. After an optimum level, further increase in rotational velocity saw a decrease in production. Also, increasing the mixture velocity increased production. It was observed that the nominal values of the operational parameters were located close to the optimum.

- Burger explained that the decrease in the production percentage due to large rotational velocities was due to the large centrifugal forces acting on the particles thus throwing them out of the cutter head. Moreover, increasing the rotational velocity increased the pump effect of the cutter head which in turn increased the outflow from the cutter head provided the suction flow was constant.

- When the rotational velocities were low, the gravitational force was dominant and because of this, particles accumulated at the lowest point of the cutter head and exited through gaps between the blades contributing to spillage. An increase in rotational velocity gave higher production due to the fact that the intensity of collisions between particles and the blades increased.

- It was observed that the particle trajectories varied according to the rotational velocity. At low rotational velocities, the particles hardly mixed and a majority of them accumulated at the lowest point of the cutter head. The particles that were sucked up, directly moved towards the suction mouth and had low residence times. Some particles were initially lifted by the blades but due to the low rotational velocity, they simply rolled over the blades and fell to the bottom of the cutter head.

- At optimum rotational velocities, a distinct flow towards the suction mouth was observed so production was higher. Many particles were lifted by the blades and they either rolled over and fell or were thrown out of the cutter head due to the centrifugal forces acting on them. At high rotational velocities, even more particles were thrown out of the cutter head due to large centrifugal forces acting on the particles. Spillage was generally higher for this case.

- In over-cutting, it was observed that the production percentage was a factor 2 to 4 lower than that in the under-cutting situation similar to actual practice. Similar to under-cutting, the production percentage increased with an increase in mixture velocity. Since not many runs were conducted in the over-cutting situation, the influence of the rotational velocity on production was not clearly found.

- Unexpectedly, the ladder angle played a crucial role in production. At high ladder angles, the negative influence of gravity was high and the particles had to travel longer distances to enter the suction mouth. Additionally, the distance between the bank and the suction mouth was greater at high angles which facilitated more water flow into the cutter head thus blocking the mixture flow towards the suction mouth.

- Alternatively, at low ladder angles, the negative influence of gravity was lower and the particles needed to travel only a small distance. Also, the distance between the bank and the suction mouth was small thus reducing the water flow into the cutter head.

Burger (2003) performed tests with varying particle diameters and noticed that the trend of the production curve was the same but the influence of the production percentage was enormous as the production percentage reduced by a factor 2 to 3. The

results plotted can be seen in Figure 10. The most likely explanations for this reduction in production percentage were the influence of gravity and the increase in particle inertia. Due to increase in particle inertia, the particles are less likely to follow the fluid and once a significant rotational velocity has been obtained, the suction flow would not be able to deflect the particle trajectory. Moreover, the increase in particle diameter had a larger influence on the production for lower rotational velocities than for the higher rotational velocities.

Also, it was observed that an initial increase in rotational velocity resulted in an increase in production. After an optimum was reached, further increase in rotational velocity caused a decrease in production. Figure 11 shows how the production percentage is influenced by the rotational velocity of the cutter head. The most likely reasons for the increase in production percentage were:

- better mixing of the particles due to collisions of particles with the blades.
- positive change of the flow within the cutter head.

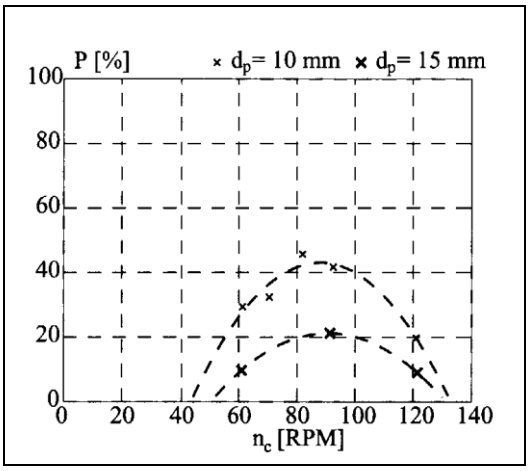

Figure 10: Influence of particle diameter on the production percentage [source: Burger (2003)]

As the rotational velocity of the cutter head increases, the intensity of collisions between the particles and the blades can also be increased. Thus, it is plausible that more particles were brought into suspension and sucked up easily. Also, a more favourable flow pattern can be obtained within the cutter head due to an increase in rotational velocity. The axial pump effect of the cutter head could have a positive effect as the axial velocities inside the cutter head are increased. Therefore, the transport of particles in the direction

of the suction pipe is increased and the probability of a particle being sucked up is increased.

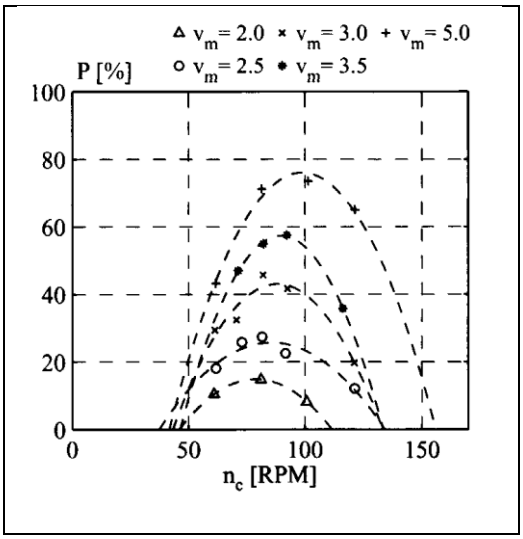

Figure 11: Production percentage vs. rotational velocity [source: Burger (2003)]

3.2 Literature on flow field around the contour of the cutter head.

In the seventies, extensive research was performed on dredge cutter performance. Dutch contractors, combined in the association CSB and Rijkswaterstaat, had performed a series of tests at and in cooperation with WL|Delft Hydraulics. The research focused on flow near and in the cutter head and on the cutting process. In all the tests, the cutter angle was maintained at 30^{o}. One of the results concerning flow inside the cutter head was:

- The cutter head worked like a combination of an axial and centrifugal pump. There was an inward flow along the contour closer to the nose of the cutter head and thus water was sucked in from the front and accelerated to the back plate. Near the back plate, an outward flow was present along the contour causing water to be thrown out of the cutter head. The combination of the axial and centrifugal pump action resulted in a flow inside the cutter head as shown in Figure 12.

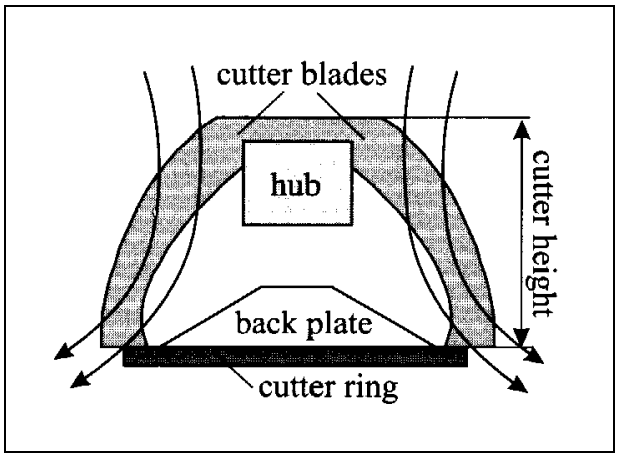

Figure 12: Combination of the axial and centrifugal pump action of the cutter head

The concept of the cutter head functioning like a combination of an axial and centrifugal pump seems viable because spillage is generally caused due to the outward flow exiting the cutter which usually occurs near the cutter ring. Thus, this study assumes that the cutter head behaves like a centrifugal pump and the numerical model will use this concept as its base.

3.3 Literature on velocity flow field within the cutter head.

Dismuke (2012) described a three-dimensional velocity flow field in the vicinity of the inlet mouth of a cutter head and tried to determine the region of influence around the cutter head by performing experiments at the Haynes Coastal Engineering Laboratory at Texas A&M. This was useful for the dredging industry as knowing the region of influence around the cutter head could help the dredge achieve higher production by using a more efficient cutting depth. The experiments involved three different suction flow rates, three different cutter head rotation speeds and two swing speeds. Dismuke (2012) found that the maximum velocities for each different flow rates were higher directly in front of the cutter head than the two planes located 30cm and 60cm away. Higher velocities were usually observed very close to the suction mouth with a rapid decrease as the distance increased.

The maximum velocities decreased with decreasing flow rate. For each flow rate, the maximum velocity 60cm from the suction mouth was approximately half of the maximum velocity observed at the plane of the suction mouth. The maximum velocities at the furthest plane were approximately 50% of the maximum velocities at the nearest

plane. Dismuke (2012) found that there was a slight decrease in the velocities near the suction inlet due to the obstruction of blades, cutter head ring and plates within the cutter head but the decrease was not significant. Under-cutting and over-cutting were performed for each scenario and it was observed that the maximum velocities greatest in the x-planes measured near to the cutter head. This was caused by the superposition of the swing speed, rotational velocity of the cutter head and suction flow rate. The rotational velocity and suction flow rate had their greatest effect near the cutter head and thus the addition of a constant swing speed increased the maximum velocities. This further proved that higher swing speed resulted in higher maximum velocities.

Dismuke (2012) noticed that there was no reduction in maximum velocities over the three distances measured when the rotational velocity was at the maximum. Even the particle settling velocity was studied in order to determine the region of influence. Initially, the velocity values were plotted at each point for all the scenarios and for each view (front, top and side), a circle or ellipse was found that enclosed all the velocities equal to or less than the maximum at each particle size. The regions were then combined into a three-dimensional model that allowed for better visualization of the region of influence. Finally, based on the skeleton provided by the region of influence from each view, an ellipsoid was formed that corresponded to the three-dimensional region of influence. Initially fine sand was used to determine the region of influence and since it was the smallest grain size used, the region of influence was larger than for other grain sizes.

3.4 Summary.

According to the tests conducted at Delft University of Technology, the residence time of particles was an important parameter that was looked into. The residence time is defined as the time from the moment the particle is injected into the cutter until the particle is sucked up by the suction mouth. The influence of the operational parameters on the residence time were observed and noted. The haul velocity (swing speed) was neglected as it was an order of magnitude lower than the rotational velocity of the cutter head and the mixture velocity and thus would not have a significant influence on the behavior of particles within the cutter head.

The filling degree of the cutter head, was introduced which indicated to what extent particle – particle interactions played a role and also how the flow was disturbed

due to the presence of particles. The filling degree was defined as the ratio between the total volume of material inside the cutter head and the internal volume of the cutter head.

An explanation was found as to why there was a lower production in the over-cut situation than the under-cut situation. Also, a simulation model was set up by representing the flow within the cutter as a superposition of a forced vortex and a sink. The force balance equation was used to obtain the equation of motion for a single particle.

Actual cutting tests were also performed by Burger (2003) in order to determine the influence of concentration of particles inside the cutter head. The influence of the operational parameters on production was noted during both the under-cutting and over-cutting cases. The particle trajectories in the two cases were studied and the influence of the rotational velocity and suction flow on them were explained. Cutting tests were conducted with varying the particle diameter and the production percentage was studied. It was observed that when the particle diameter was increased, the production percentage reduced by a factor of 2 to 3.

Tests conducted at the Haynes Coastal Engineering Laboratory at Texas A&M were used to describe a three-dimensional velocity flow field in the vicinity of the suction mouth. Using this information, the region of influence around the cutter head was determined. The experiments involved three different suction flow rates, three different cutter head rotation speeds and two swing speeds. It was found that the maximum velocities for each different flow rates were higher directly in front of the cutter head than away from it.

Even the particle settling velocity was studied in order to determine the region of influence. Initially, the velocity values were plotted at each point for all the scenarios and for each view (front, top and side), a circle or ellipse was found that enclosed all the velocities equal to or less than the maximum at each particle size. The regions were then combined into a three-dimensional model that allowed for better visualization of the region of influence. Finally, based on the skeleton provided by the region of influence from each view, an ellipsoid was formed that corresponded to the three-dimensional region of influence.

Also, from experiments conducted in the seventies, it was observed that the cutter head behaved like a combination of an axial and centrifugal pump. Hence for the remainder of this study, the cutter head is assumed to behave like a centrifugal pump.

4

Methodology

4.1 Introduction.

As mentioned in the previous chapter, from experiments conducted in the seventies the cutter head is observed to function as a combination of an axial and centrifugal pump. Inspired by Nieuwboer (2017), Miedema (2017) came up with an approach which is used as the base for this numerical model. The model states that near the nose of the cutter head, there is a flow directed inwards along the contour of the cutter head and this flow is responsible for the mixture of sand and water to enter the cutter head. This incoming flow is a combination of the cutting production and water. Similarly, near the cutter ring, there is a flow directed outwards along the contour of the cutter head and this flow is responsible for the mixture to exit the cutter head and in turn responsible for spillage. Thus, calculating this outgoing flow will pretty much provide a value for spillage.

4.2 Methodology.

Since a numerical model has not been developed to date, no reference is available to base this model upon. Therefore, a new approach has been assumed as the base for this numerical model. Since there is an inflow close to the nose and an outflow close to the cutter ring of the cutter head, a distinct separation between the two flows is difficult to estimate. Hence, Miedema (2017) divided the cutter head into two slices with the top slice having an inflow and the bottom slice having an outflow. Since the cutter head is assumed to behave like a centrifugal pump then each slice will behave like an individual pump.

The top slice is named as slice 2 and the bottom slice as slice 1. The parameters in slice 2 are:

w_2 = height of the slice.

p_2 = pressure within the slice.

Q_2 = flow within the slice.

D_2 = average diameter of the slice.

Similarly, slice 1 will have the corresponding parameters w_1, p_1, Q_1 and D_1.

The region close to the nose of the cutter is slice 2 and thus the flow Q_2 should be an inflow. Figure 13 shows the diagram of a cutter head depicting the flows involved. Miedema (2017) further states that the inflow in slice 2 is caused due to the pump action and due to this, the flow is accelerated to the back plate. The presence of the suction mouth within the cutter head is also responsible for this inflow. The outflow at the cutter ring is also caused due to the pump action and is intensified due to the centrifugal force brought about by the rotation of the cutter head. If the suction flow is kept constant, an increase in the inflow will correspondingly cause an increase in the outflow.

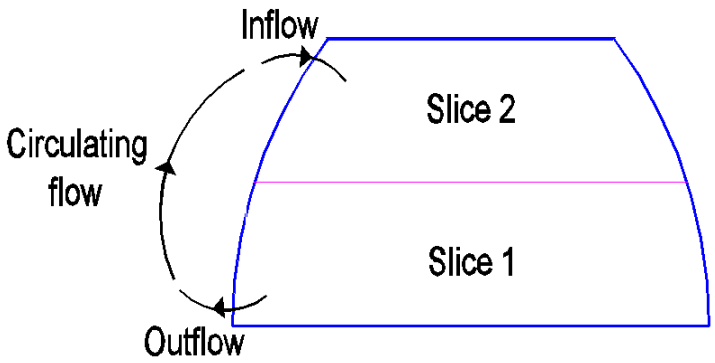

Figure 13: Diagram of a cutter showing the flows involved

Miedema (2017) states that this approach assumes the outward flow from slice 1 (Q_1) is a circulating flow which re-enters the cutter through slice 2. Although the flow circulates back into the cutter head, the particles leaving the cutter head will not return. Only water re-enters the cutter head as the inflow in slice 2. It is assumed that only water is present in slice 2 and thus the density involved is that of water. Whereas, the particles

and water combine to form a mixture as it moves along the cutter head and thus the density involved in slice 1 is that of the mixture.

Since the diameter in slice 1 is greater than that in slice 2, the velocity in slice 2 will be greater than the velocity in slice 1 (due to the continuity equation) and thus by Bernoulli's law, the pressure p_1 should be greater than p_2. Also, due to the presence of the suction mouth, pressure p_1 will be high pressure.

The equations for pressure and flow are derived using the pump affinity laws. Affinity laws of a centrifugal pump express the effect on pump performance due to changes in certain application variables. The variables that affect pump performance are the pump speed and impeller diameter. The affinity laws are derived from a dimensional analysis of three important parameters that describe pump performance namely flow, total head and power. The analysis is based on the reduced impeller being geometrically similar and operated at dynamically similar conditions or equal specific speed. If that is the case then the affinity laws can be used to predict the performance of the pump at different diameters for the same speed or different speed for the same diameter (Karassik et al. 2001).

In order to derive the affinity laws, non-dimensional parameters are used. One such parameter is the discharge coefficient (C_D). The discharge coefficient is defined as the ratio of the actual discharge to the theoretical discharge, i.e.

$$C_D = \frac{Q}{nD^3}$$

where, n = rotational velocity of impeller in rps.

D = diameter of impeller in m.

Q = flow rate in m^3/s.

Performing the dimensional analysis shows that both the numerator and the denominator on the right-hand side of the equation has a unit of m^3/s. Thus, the discharge coefficient is a non-dimensional parameter. This also means that the flow rate, rotational velocity and impeller diameter at one operating point is equal to the corresponding parameters at another point.

$$\frac{Q_1}{n_1 {D_1}^3} = \frac{Q_2}{n_2 {D_2}^3}$$

This allows us to make a relationship between the discharge flow rate and speed of the pump as well as the discharge flow rate and the impeller diameter, i.e.

$$\frac{Q_1}{n_1} = \frac{Q_2}{n_2}$$

$$\frac{Q_1}{{D_1}^3} = \frac{Q_2}{{D_2}^3}$$

Re-arranging these equations gives one part of the affinity laws.

$$\frac{Q_1}{Q_2} = \frac{n_1}{n_2} = \frac{{D_1}^3}{{D_2}^3}$$

This comes in handy when one flow rate and one operating speed is known and when the second operating speed needs to be calculated at which the second flow rate can be achieved. Also, if the flow rates that are given and that needs to be achieved are known then the impeller diameter can be altered to achieve the required flow rate. Similarly, another parameter used is the head coefficient (C_H).

$$C_H = \frac{gH}{n^2 D^2}$$

where, g = acceleration due to gravity in m/s^2.

H = pump head in m.

n = rotational velocity of impeller in rps

D = impeller diameter in m.

Once again, performing the dimensional analysis shows that both the numerator and denominator of the right-hand side of the equation have the same unit (m^2/s^2). Thus, the head coefficient is a non-dimensional parameter. Therefore,

$$\frac{gH_1}{{n_1}^2 {D_1}^2} = \frac{gH_2}{{n_2}^2 {D_2}^2}$$

This allows us to make a relationship between pump head and operating speed of pump as well as the pump head and the impeller diameter, i.e.

$$\frac{H_1}{{n_1}^2} = \frac{H_2}{{n_2}^2}$$

$$\frac{H_1}{{D_1}^2} = \frac{H_2}{{D_2}^2}$$

Re-arranging these equations gives another part of the affinity laws.

$$\frac{H_1}{H_2} = \frac{{n_1}^2}{{n_2}^2} = \frac{{D_1}^2}{{D_2}^2}$$

This comes in handy when one pump head and one operating speed is known and when the second operating speed needs to be calculated at which the second pump head can be achieved. Also, if the pump heads that are given and that needs to be achieved are known then the impeller diameter can be altered to achieve the required pump head. Thus, the affinity laws are:

$$\frac{Q_1}{Q_2} = \frac{n_1}{n_2} = \frac{{D_1}^3}{{D_2}^3} \quad (1)$$

$$\frac{H_1}{H_2} = \frac{{n_1}^2}{{n_2}^2} = \frac{{D_1}^2}{{D_2}^2} \quad (2)$$

It can be seen that the discharge flow rate Q is related to the rotational velocity n and the cube of the impeller diameter. Hence, a relation can be formulated:

$$Q \propto nD^3$$

For a radial discharge impeller, the impeller meridional exit area is the product of the impeller diameter (D) and the width of the blades (b) (Karassik et al. 2001). Hence,

$$Q \propto nD^2b$$

Figure 14 shows the diagram of a cutter head with a geometry of a truncated cone. In terms of a cutter head,

H = head of the slice.

n = rotational velocity of the cutter.

D = diameter of the slice.

w = height of the slice.

Q = flow through the slice.

ϕ = blade angle within the slice.

Therefore, the equation for Q becomes:

$$Q \propto nD^2w$$

In the base model (Appendix B) proposed by Miedema (2017), the parameters involved in the model are the height of the cutter head w, the height of the two slices w_1 and w_2, the pressures p_1 and p_2, flows Q_1 and Q_2, the mixture flow Q_m and the diameters D_1 and D_2. In order to improve the base model, additional parameters are incorporated into it. Firstly, the blade angle is included in the equation of flow. The reason behind this is because the blade angle influences the flow into or out of the cutter head. The orientation of the blade of a cutter head determines the area of the gap between the blades. Hence, the larger the area, the larger will be the flow through the slice.

Incorporating the blade angle of the cutter head evolves the relation to:

$$Q \propto nD^2w \tan\varphi$$

$$Q = \beta nD^2w \tan\varphi \qquad (3)$$

where, β = a constant of proportionality.

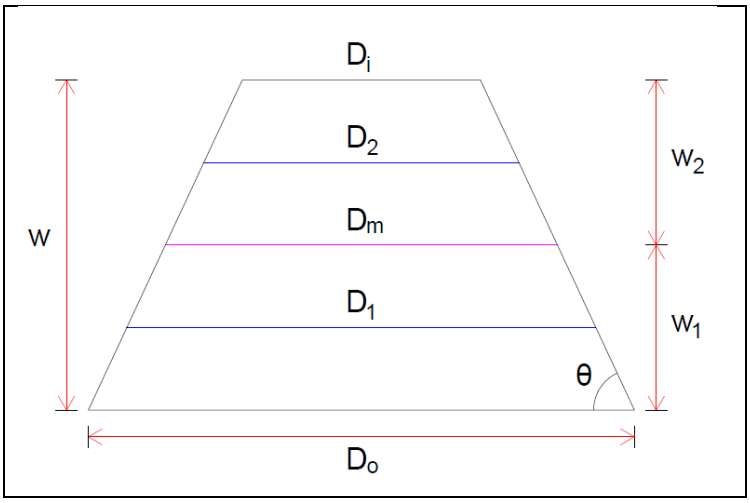

Figure 14: Diagram of a cutter head.

The blade angle is taken as the angle between the line drawn along the inner side of the blade and the tangent to the cutter diameter drawn at the midpoint of the blade (Talmon 2010). Figure 15 shows a diagram of how the blade angle is obtained. The blade angle in each slice is taken at the average diameters (D_1 & D_2) of each slice. The diameters D_1 and D_2 are functions of the height of the bottom slice (w_1). This means that as w_1 varies in the model, the diameters D_1 and D_2 will vary accordingly which in turn will vary the blade angles in each slice. For simplicity, the blade angles are taken when the height of the bottom slice is half the height of the cutter head, i.e. $w_1=w/2$.

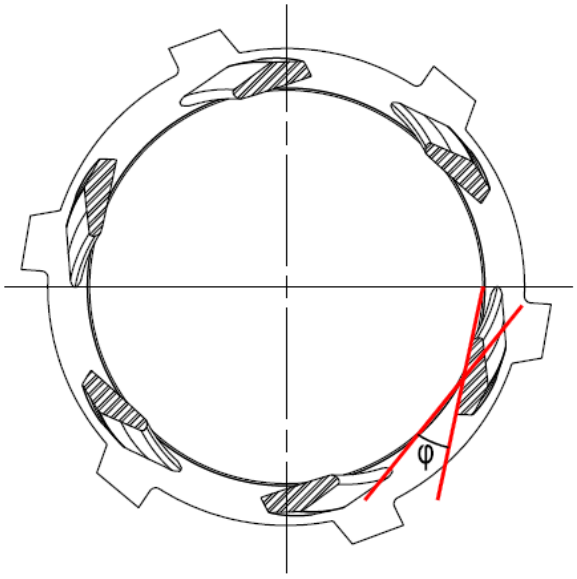

Figure 15: Blade angle of a cutter

The diameters D_1 and D_2 are made functions of the height of the bottom slice w_1 by assuming the cutter head geometry to be that of a truncated cone with a cutter angle θ (constant slope). Since D_1 and D_2 are unknowns, they are linked with the diameter at the cutter ring D_o and the diameter at the nose D_i which are known. Using the concept of right-angled triangles, D_1 and D_2 are made functions of D_o, D_i, w_1 and θ. The cutting production Q_p is incorporated into the equation because it accounts for the particles entering the cutter head. For the simple case, the cutting production is defined as the product of the cut face (depth of cut), the step size and the swing speed. Hence, these three parameters are also added to the model.

Since the cutter head deals with pressure, the head H can be converted to pressure p by the following relation

$$gH = \frac{p}{\rho}$$

It can be seen that the pressure is related to the square of the rotational velocity and square of the diameter. Hence a relation can be formulated:

$$p \propto n^2 D^2 \rho$$

$$p = \alpha n^2 D^2 \rho \qquad (4)$$

where, ρ = density.

α = a constant of proportionality.

A relationship between flow Q and pressure p can be obtained by utilizing the specific flow. The specific flow is defined as the volumetric flow per unit length, i.e

$$q = \frac{Q}{w} \qquad (5)$$

(3) can be re-written as:

$$\frac{Q}{w} = \beta n D^2 \tan\varphi \qquad (6)$$

Now substitute (6) in (5):

$$q = \frac{Q}{w} = \beta n D^2 \tan \varphi \tag{7}$$

Also, (4) can be re-written as:

$$\frac{p}{\alpha n \rho} = nD^2 \tag{8}$$

Now substitute (8) in (7):

$$q = \frac{Q}{w} = \beta \frac{p}{\alpha n \rho} \tan \varphi \tag{9}$$

So,

$$q = \frac{\beta}{\alpha n \rho} p \tan \varphi \tag{10}$$

And

$$Q = \frac{\beta}{\alpha n \rho} p w \tan \varphi \tag{11}$$

Since the cutter head is assumed to be split into 2 slices, with the bottom slice (at the back ring) as 1 and the top slice (near the nose) as 2, the respective pressures and flows for both slices can be found.

For slice 1,

$$p_1 = \alpha n^2 {D_1}^2 \rho_1 \tag{12}$$

$$Q_1 = \frac{\beta}{\alpha n \rho_1} p_1 w_1 \tan \varphi_1 \tag{13}$$

It is assumed that in slice 1, both particles and water combine to form a mixture and thus the density in this slice is ρ_1. But in slice 2, it is assumed that the incoming flow consists only of water and thus the density in this slice is ρ_2.

For slice 2,

$$p_2 = \alpha n^2 {D_2}^2 \rho_2 \tag{14}$$

$$Q_2 = (q_2 - q_1) w_2 \tag{15}$$

$$Q_2 = \frac{\beta}{\alpha n \rho_2} (p_2 - p_1) w_2 \tan \varphi_2 \tag{16}$$

Since the top slice (slice 2) has an inflow then the flow Q_2 is an inward flow. Similarly, since the bottom slice (slice 1) has an outflow then the flow Q_1 is an outward flow. The mixture flow Q_m is defined as the flow through the suction mouth and since it exits the cutter head, it is therefore considered as an outward flow whereas the cutting production Q_p is defined as the flow of material that is cut from the seabed and since it enters the cutter head, it is considered as an inward flow.

In order to formulate an equation, all outgoing flows are considered positive and all incoming flows are considered negative (Miedema 2017). The flow is assumed to be incompressible and thus, the combination of the densities at the inflow is accounted for at the outflow. The continuity equation states that for an incompressible flow, the volume flow rate of the inflow is equal to the volume flow rate at the outflow. In other words, the sum of all flows is equal to 0,

$${Q_1}^{(+)} + {Q_2}^{(-)} + {Q_m}^{(+)} + {Q_p}^{(-)} = 0 \tag{17}$$

$$Q_1 + Q_2 + \left(Q_m - Q_p\right) = 0$$

Substituting (13) and (16) in the above equation gives,

$$\frac{\beta}{\alpha n \rho_1} p_1 w_1 \tan \varphi_1 + \frac{\beta}{\alpha n \rho_2} (p_2 - p_1) w_2 \tan \varphi_2 + \left(Q_m - Q_p\right) = 0$$

$$\frac{\beta}{\alpha n}\left(\frac{p_1 w_1 \tan\varphi_1}{\rho_1}+\frac{(p_2-p_1)w_2\tan\varphi_2}{\rho_2}\right)+(Q_m-Q_p)=0$$

$$\frac{p_1 w_1 \tan\varphi_1}{\rho_1}+\frac{(p_2-p_1)w_2\tan\varphi_2}{\rho_2}+\frac{\alpha n}{\beta}(Q_m-Q_p)=0$$

$$\frac{p_1 w_1 \tan\varphi_1}{\rho_1}=\frac{(p_1-p_2)w_2\tan\varphi_2}{\rho_2}-\frac{\alpha n}{\beta}(Q_m-Q_p)$$

$$w_1=\left(\frac{p_1-p_2}{p_1}\right)w_2\frac{\tan\varphi_2}{\tan\varphi_1}\frac{\rho_1}{\rho_2}-\frac{\alpha n\rho_1}{\beta}\frac{(Q_m-Q_p)}{p_1\tan\varphi_1} \quad (18)$$

Substituting (12) and (14) in (18) gives,

$$w_1=\left(\frac{{D_1}^2\rho_1-{D_2}^2\rho_2}{{D_1}^2\rho_1}\right)w_2\frac{\tan\varphi_2}{\tan\varphi_1}\frac{\rho_1}{\rho_2}-\frac{1}{\beta n{D_1}^2\tan\varphi_1}(Q_m-Q_p) \quad (19)$$

In order to simplify the equation, let's say:

$$f=\left(\frac{{D_1}^2\rho_1-{D_2}^2\rho_2}{{D_1}^2\rho_1}\right)$$

$$C=\frac{\tan\varphi_2}{\tan\varphi_1}$$

$$a=\frac{\rho_1}{\rho_2}$$

Thus, (19) simplifies to:

$$w_1=fw_2Ca-\frac{1}{\beta n{D_1}^2\tan\varphi_1}(Q_m-Q_p)$$

$$w_1=f(w-w_1)Ca-\frac{1}{\beta n{D_1}^2\tan\varphi_1}(Q_m-Q_p)$$

$$w_1(1+fCa)=wfCa-\frac{1}{\beta n{D_1}^2\tan\varphi_1}(Q_m-Q_p)$$

$$w_1 = \frac{wfCa - \frac{1}{\beta n {D_1}^2 \tan \varphi_1}(Q_m - Q_p)}{1 + fCa} \quad (20)$$

where, w = height of the cutter head

f = $\frac{{D_1}^2\rho_1 - {D_2}^2\rho_2}{{D_1}^2\rho_1}$

C = $\frac{\tan \varphi_2}{\tan \varphi_1}$

a = $\frac{\rho_1}{\rho_2}$

β = a constant

n = rotational velocity of the cutter head (rps)

D_1 = diameter of slice 1 (m)

ϕ_1 = blade angle in slice 1

Q_m = mixture flow at the suction mouth

Q_p = cutting production

Although the diameters D_1 and D_2 are average diameters of slices 1 and 2 respectively, they will vary according to the height of slice 1 w_1. Therefore, these two diameters are made a function of w_1. The relation between diameters D_1, D_2 and w_1 is derived by using the theorem of right angles triangles in the below diagrams.

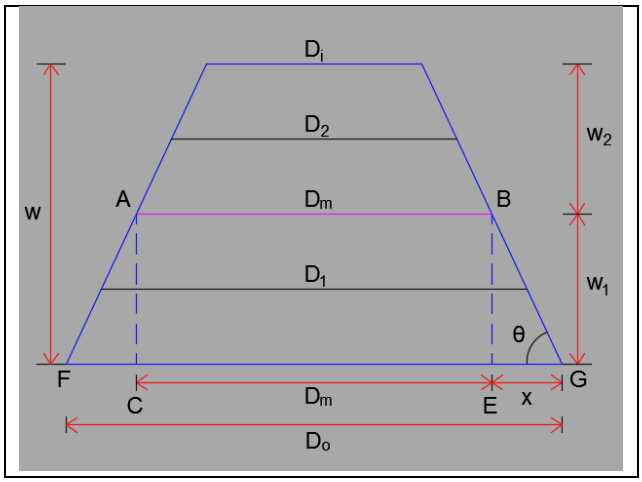

(a)

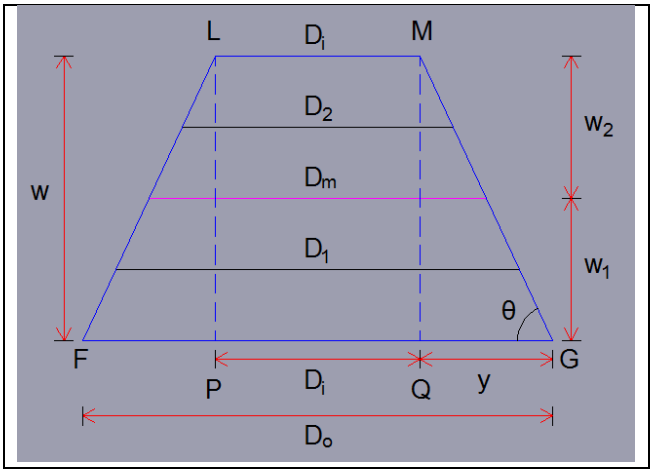

(b)

Figure 16: Relation between D_1, D_2 and w_1 using the concept of right angled triangles.

Figure 16(a) is used to derive a relation between diameter of bottom slice D_1 and the height of the bottom slice w_1. Consider ΔBEG, using the concept of right angled triangles

$$\tan\theta = \frac{w_1}{x}$$

$$x = \frac{w_1}{\tan\theta}$$

If D_o is the diameter at the cutter ring and D_m is the diameter at the interface of the slices then,

$$D_o = D_m + 2x$$

$$D_m = D_o - \frac{2w_1}{\tan\theta} \tag{21}$$

Diameter D_1 is the average diameter in slice 1, therefore

$$D_1 = \frac{D_o + D_m}{2}$$

$$D_1 = \frac{D_o + D_o - \frac{2w_1}{\tan\theta}}{2}$$

$$D_1 = D_o - \frac{w_1}{\tan\theta} \tag{22}$$

Figure 16(b) is used to derive a relation between diameter of the top slice D_2 and height of the bottom slice w_1. Consider ΔMQG and using the concept of right angled triangles,

$$\tan\theta = \frac{w}{y}$$

$$y = \frac{w}{\tan\theta}$$

Now D_i is the diameter of the cutter head at the nose hence,

$$D_o = D_i + 2y$$

$$D_o = D_i + \frac{2w}{\tan\theta} \tag{23}$$

Diameter D_2 is the average diameter in slice 2, therefore

$$D_2 = \frac{D_i + D_m}{2}$$

$$D_2 = \frac{D_i + D_o - \frac{2w_1}{\tan\theta}}{2}$$

$$D_2 = \frac{D_i + D_i + \frac{2w}{\tan\theta} - \frac{2w_1}{\tan\theta}}{2}$$

$$D_2 = D_i + \frac{(w - w_1)}{\tan\theta} \quad (24)$$

If (22) and (24) are substituted in (20), it can be seen that (20) has the term w_1 on either side of the equation and is therefore an implicit equation. Thus, an iteration is required to calculate the value of w_1. In the model, a random value of w_1 is used in the right-hand side of equation (20) and is called 'start value'. Using this start value of w_1, a value for w_1 is calculated by using (20) and this is called the 'calculated value'. A 'check cell' is created to calculate the difference between the start value and the calculated value. Hence, the model continues to iterate until the value of the check cell becomes 0. The model uses the following code for the iteration.

Range("check cell").GoalSeek Goal:=0, ChangingCell:=Range("start value")

Once the value of w_1 is calculated, the outgoing flow Q_1 (also called circulating flow Q_c) can be calculated using (3)

$$Q_c = Q_1 = \beta n {D_1}^2 w \tan\varphi$$

The total outgoing flow can now be defined as,

$$Q_T = Q_c + Q_m$$

Therefore, spillage is now defined as the ratio of circulating flow to the total outgoing flow and is given by the relation:

$$Spillage = \frac{Q_c}{Q_T}$$

The model can be modified to incorporate a cylindrical cutter head with the cutter angle being 90^o implying that the diameter at the cutter ring D_o and the diameter at the nose D_i are equal. The model provides a spillage of about 40%. This value is not accurate because the physics involved with a cylindrical cutter head differs from that of a general cutter head. The pump effect will not be present in the case of a cylindrical cutter head and thus, this model cannot be used.

4.3 Summary.

From experiments conducted in the seventies, it was observed that the cutter head behaved like a combination of an axial and centrifugal pump, implying that there is an inflow close to the nose of the cutter head which propels the flow to the back plate and there is an outflow that resulted in the region close to the cutter ring of the cutter head. This is taken as the base for the numerical model and so the cutter head is divided into two slices with each slice assumed to behave like an individual pump. Hence the pump affinity laws are defined and are used to derive equations for the pressure and flow associated with the cutter head.

The theory states that once the flow enters the cutter head near the nose, it is propelled to the cutter ring where an outflow is present. This outflow circulates back into the top slice as the inflow. The most important parameter is the height of the bottom slice w_1 because other parameters are dependent on it. Thus, an equation for w_1 is obtained after simplification. An iteration process is done to calculate the value of w_1 and thus the circulating flow is calculated. Ultimately spillage is estimated as the ratio of the circulating flow to the total outgoing flow.

5

Execution of model - Results

As mentioned in the previous chapter, the height of slice 1 (w_1) is the most important variable in the model since the other variables are dependent on it. Hence, an equation for w_1 is obtained:

$$w_1 = \frac{wfCa - \frac{1}{\beta n {D_1}^2 \tan\varphi_1}(Q_m - Q_p)}{1 + fCa}$$

5.1 Input variables.

Each dredge has its own characteristic specifications and the type of cutter head is also dependent on those specifications. For the current model, the dredge is a cutter suction dredge called 'The Texas' which belongs to Great Lakes Dredge & Dock (GLDD) and it is generally used to cut sand. The known parameters of the cutter head are fed as input to the model.

The height of the cutter head (w) is known and so is the diameter at the cutter ring (D_o). Although the diameter at the nose of the cutter is known, D_i is calculated using the equation below because the cutter is assumed to be in the form of a truncated cone.

$$D_i = D_o - \frac{2w}{\tan\theta}$$

where, θ = angle of the cutter head (constant slope).

The rotational velocity of the cutter head (n) is known and is generally maintained at a constant value. The value for β is calibrated from real life data obtained from The Texas (GLDD) in one of its projects. The suction flow (Q_m) is a known quantity and is based

on the dredge pump. As mentioned, these parameters are exclusive for The Texas and these will change depending on the dredge that is used as the reference for the model.

Also, the cutting production can be fed as an input. The cutting production (Q_p) is defined as the amount of material that is cut from the seabed and enters the cutter head. It can be calculated as follows:

$$Q_p = F_{cut} S v_{swing}$$

where, F_{cut} = cut face (depth of cut).

S = step size.

v_{swing} = swing speed of the cutter.

The cut face and step size can vary depending on project estimates and goals. The swing speed is also fed as input. The blade angles are calculated from the two slices as explained in Figure 15. The cutter angle will be constant since the cutter head is assumed to be in the form of a truncated cone with constant slope.

5.2 Calibration.

Initially, the values of the input parameters used in the model are assumed (Miedema 2017). These parameters and values are:

Height of the cutter head, w = 2.5 m

Diameter in slice 1, D_1 = 3 m

Diameter in slice 2, D_2 = 2 m

Rotational velocity, n = 0.5 rps

Flow in suction pipe, Q_m = 2.736 m^3/s

The value of β is assumed to be 1.2. Using these values, height of the bottom slice, w_1 is found to be 0.16 m and the spillage is 18.1%. Thus, to calibrate the value of β, these initial values are used but the spillage is taken from real-life data values obtained from the hydrographic surveys of The Texas.

From the hydrographic surveys, a wide range of spillage values is obtained ranging from 20% – 34% (See Appendix A). Hence, for simplicity, the average of this range of spillage is used to calibrate the value of β which is 27%. Now, since the spillage is known, the process is "reverse-engineered" to calculate the value of β.

Spillage = 27% = 0.27

Using the equation of spillage:

$$Spillage = \frac{Q_c}{Q_c + Q_m}$$

The value of Q_c is obtained to be 1.01 m^3/s. If the equation of Q_c is utilized, then the β value can be calculated, i.e.

$$Q_c = \beta n {D_1}^2 w$$

Substituting the values of the parameters mentioned, a β value of 1.4 is obtained. Hence, this value is used for the remainder of the study.

5.3 Results.

For the model, real life data from The Texas (GLDD) is used. Thus, all the values corresponding to the dredge (dimensions and operational parameters) are exclusive only to cutter head of The Texas. Table 1 shows the dimensions of the cutter head that is used for the analysis.

Parameters	Values used
Height of the cutter, w	1.6 m
Diameter at the back ring, D_o	2.48 m
Diameter at the nose, D_i	0.78 m
Blade angle (slice 1), ϕ_1	28°
Blade angle (slice 2), ϕ_2	38°
Cutter angle	62°

Table 1: Cutter dimensions of The Texas.

The cutter head used in this example is one of the smaller cutter heads. The diameter at the back ring is the largest diameter of the cutter head and the diameter at the nose is the smallest diameter. Since the geometry of the cutter head is assumed to be a truncated cone, a constant slope is assumed. Table 2 shows the operational parameters of the cutter suction dredge that are used for the analysis.

Parameters	Values used
Rotational velocity, n	30 rpm
Flow in suction pipe, Q_m	2.1 m^3/s
Cutting production, Q_p	0.686 m^3/s
Cut face, F_{cut}	1.5 m
Step size, S	1.5 m
Swing speed, v_{swing}	0.305 m/s

Table 2: Operational parameters of The Texas

For the analysis, the rotational velocity, suction flow and swing speed of the cutter head are varied to observe their influence on spillage. Ideally the suction flow is kept at a constant. The cut face is generally varied depending on the target depth to be achieved. Table 3 shows the constants and calculated values used in the model.

The model estimates spillage to be around 38%. From the hydrographic surveys, spillage while cutting sand is in the range of 20 – 34%. Therefore, the value obtained is close to the actual values obtained in practice.

Parameters	Values used
Beta, β	1.40
C	1.469
Factor, f	0.816
Diameter, D_1^2	4.715 m^2
Diameter, D_2^2	1.422 m^2
Height of slice 1, w_1	0.821 m
Height of slice 2, w_2	0.779 m
Circulating flow, Q_c	1.28 m^3/s
Spillage	37.80%

Table 3: Constants and calculated values of The Texas.

5.4 Sensitivity analysis.

For the sensitivity analysis, some of the operational parameters of The Texas are compared with spillage in order to understand the effects they have on spillage but first the β value is used to check the corresponding spillage values obtained. Figure 17 shows the influence of β on spillage. It can be seen that spillage increases as the β value increases (logarithmic growth). Logarithmic growth means that initially the increase in spillage with respect to β will be great but after a certain value of β, the increase in spillage with respect to β will continue to get smaller.

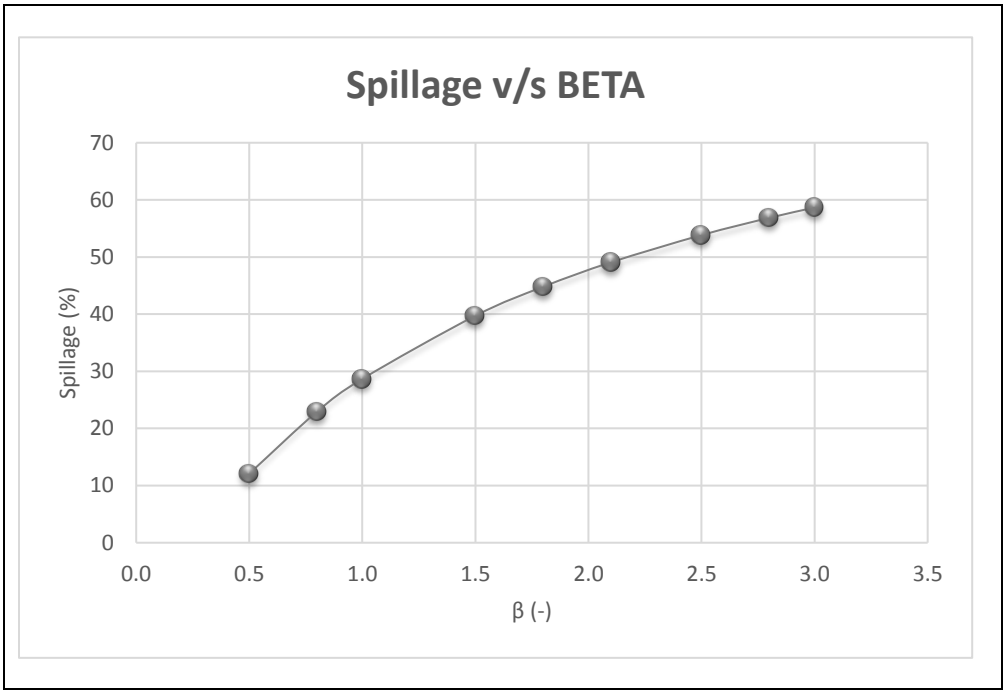

Figure 17: Relationship between spillage and beta.

For the current model, a β=1.4 is used to obtain spillage. As mentioned earlier, a sensitivity analysis is performed on the operational parameters. In order to observe the behaviour of the operational parameters, different β values are used (β=1, β=1.4 and β=2). Figure 18 shows how the suction flow influences spillage. It can be seen that increasing the suction flow will drastically reduce spillage but the question is: "Is this feasible?". In practice, the answer is no because although spillage can be reduced other parameters will be forced to increase.

Increasing the suction flow means that the pump should have a higher capacity to match the suction flow. This in turn requires more power to run the pump which will then bring cost into the equation. Ideally, dredging companies would prefer to have an optimum value for suction flow which would lower spillage but also keep the price tag to the minimum.

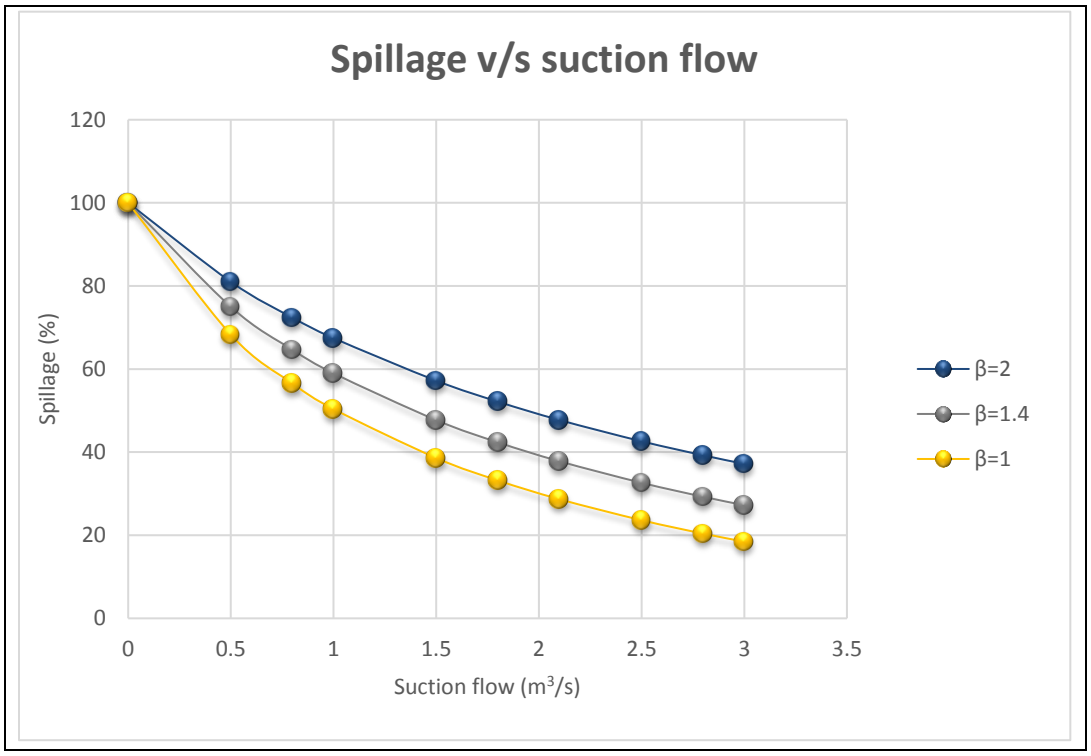

Figure 18: Relationship between spillage and suction flow within the suction mouth

The next parameter compared with spillage is the rotational velocity of the cutter. Figure 19 shows how the rotational velocity of the cutter influences spillage. At low rotational velocities, the spillage is quite low as should be the case since a low rotational velocity implies low centrifugal forces acting on the particles within the cutter head. A low rotational velocity also implies a low production as the material pick-up will be low.

As the rotational velocity increases, the spillage begins to increase and the reason for this is because of the large centrifugal forces present due to the high rotational velocities. It is obvious from this graph that high rotational velocities are undesirable due to increased spillage but employing low rotational velocities would have an adverse effect since production will be reduced.

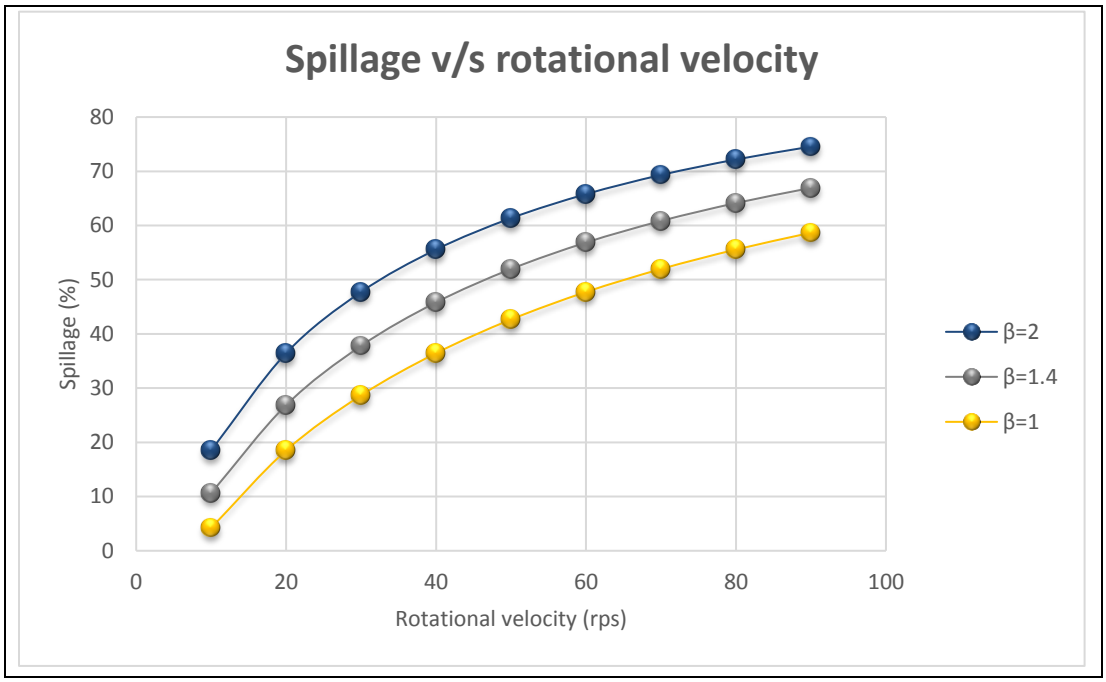

Figure 19: Relationship between spillage and rotational velocity of cutter

Burger (2003) conducted experiments and found that an initial increase in rotational velocity resulted in an increase in production but after a certain optimum was reached, any further increase in the rotational velocity resulted in a decrease in production. Figure 11 shows the graph obtained from Burger's experiments. Hence, an optimum value of rotational velocity is desired wherein spillage is reduced without sacrificing production.

The swing speed of the cutter is also used to compare with spillage. Figure 20 shows how the swing speed influences spillage. As seen from the graph, increasing the swing speed of the cutter head slightly increases spillage (linear increase). This means that the swing speed is not a major contributor to spillage when compared with the suction flow and the rotational velocity of the cutter. Increasing the swing speed creates a bull-dozing effect by which materials are forcibly pushed along the seabed. In this case, spillage is mostly caused due to the slice thickness of the cut material being greater than the gap between the blades thus making it unable for the material to enter the cutter head.

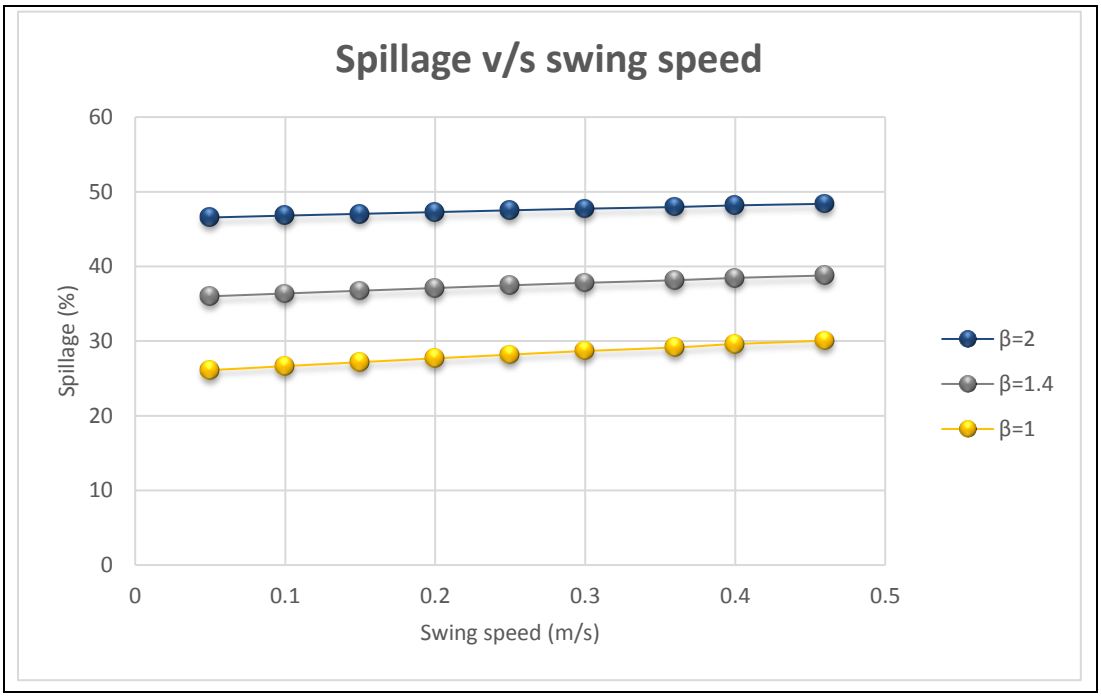

Figure 20: Relationship between spillage and swing speed of the cutter

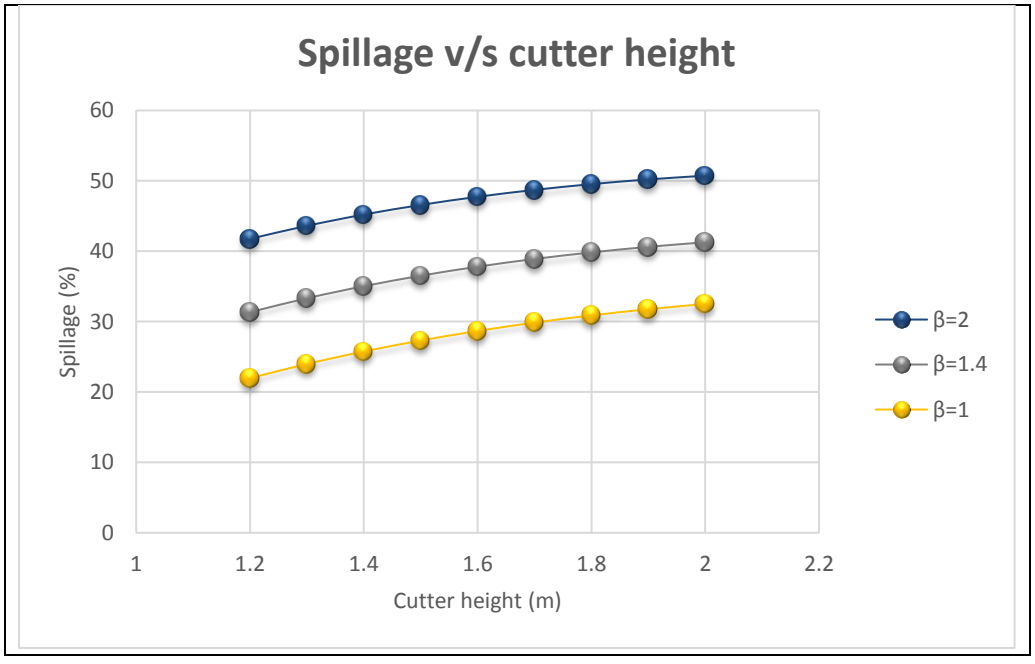

Figure 21: Relationship between spillage and cutter head height.

The cutter head height w is compared with spillage as shown in Figure 21. It can be seen that as the cutter head height increases, spillage increases as well (almost linear increase). The reason for this increase is due to the fact that as the cutter head height increases, the heights of the bottom slice as well as the top slice varies. An increase in either w_1 or w_2 will affect the outflow thus increasing spillage since the suction flow rate is kept constant.

5.5 Summary.

Real life data are taken from The Texas (GLDD) as the input parameters of the cutter head. The model estimated spillage to be about 38% and when compared to the spillage values seen in the industry, this value is in close proximation. Hence the model provides a realistic value for spillage.

Also, sensitivity analysis is performed on the model with parameters such as the rotational velocity, suction flow and the swing speed of the cutter head and plotted as graphs. The relationship of these parameters with spillage were in line with what is observed in practice. Hence it can be said that the model, although simple, does work as intended. Another important parameter used for the sensitivity analysis is the constant β that influences the flow. Various β values are used to see their influence on the relationship between the operational parameters and spillage. The validation of the model is discussed in the next chapter.

6

Validation of the model

6.1 Introduction.

Unfortunately, experiments were unable to be conducted which would have helped to validate the model more accurately. Thus, the hydrographic surveys obtained from The Texas during one of its projects are used to validate this model. The surveys are taken at different dredging locations and from these surveys the production and spillage can be obtained by drawing a contour. Although this method does not seem to be overly accurate, this is the best way to compare results between real-life projects and the output from the model.

Figure 22 shows a seabed that has been dredged. The cutting depth is the depth at which the cutter head cuts. The before-dredging depth, as the name implies, is the depth of the seabed before any dredging operation commences. The after-dredging depth is the depth achieved after dredging operations have been completed. Here, spillage is defined as the difference in elevation between the cutting depth and the after-dredging depth.

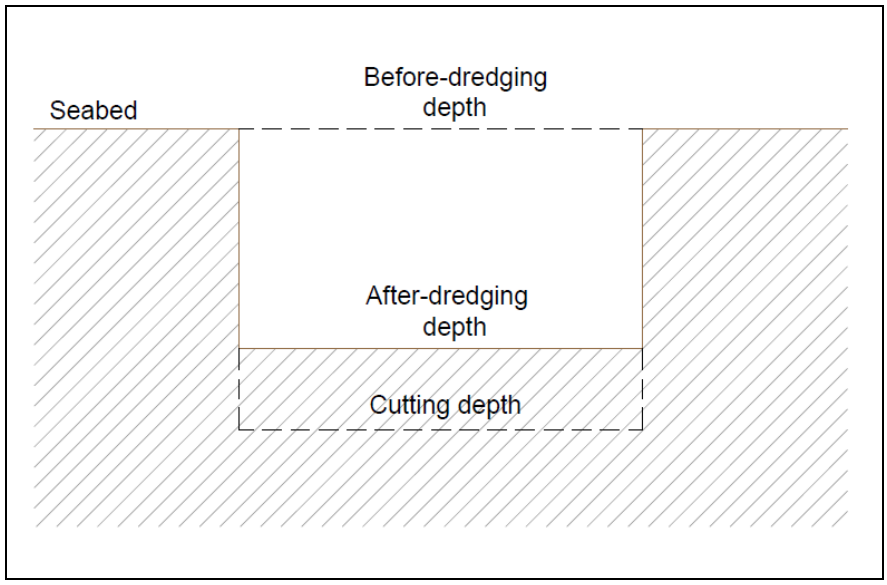

Figure 22: Diagram of a dredged seabed showing the various elevations.

6.2 Validation.

Figure 23 shows the hydrographic survey that is obtained from location '40+00' of 'Cut 4'. The contour highlighted shows the cutting production and if this contour is measured, an area of about 18.66 m^2 is obtained. Similarly, in the same survey of 'Cut 4', the production (amount of material that enters the suction mouth) can be measured. This is shown by the contour in Figure 24 and measures about an area of 12.22 m^2. Using these two areas, the area of the spillage contour can be obtained, i.e. spillage = cutting production – actual production which gives an area 6.44 m^2. Now the percentage of spillage is basically the ratio of the amount of spillage to the cutting production, i.e. spillage (%) = spillage/cutting production which gives a value of 34.5%.

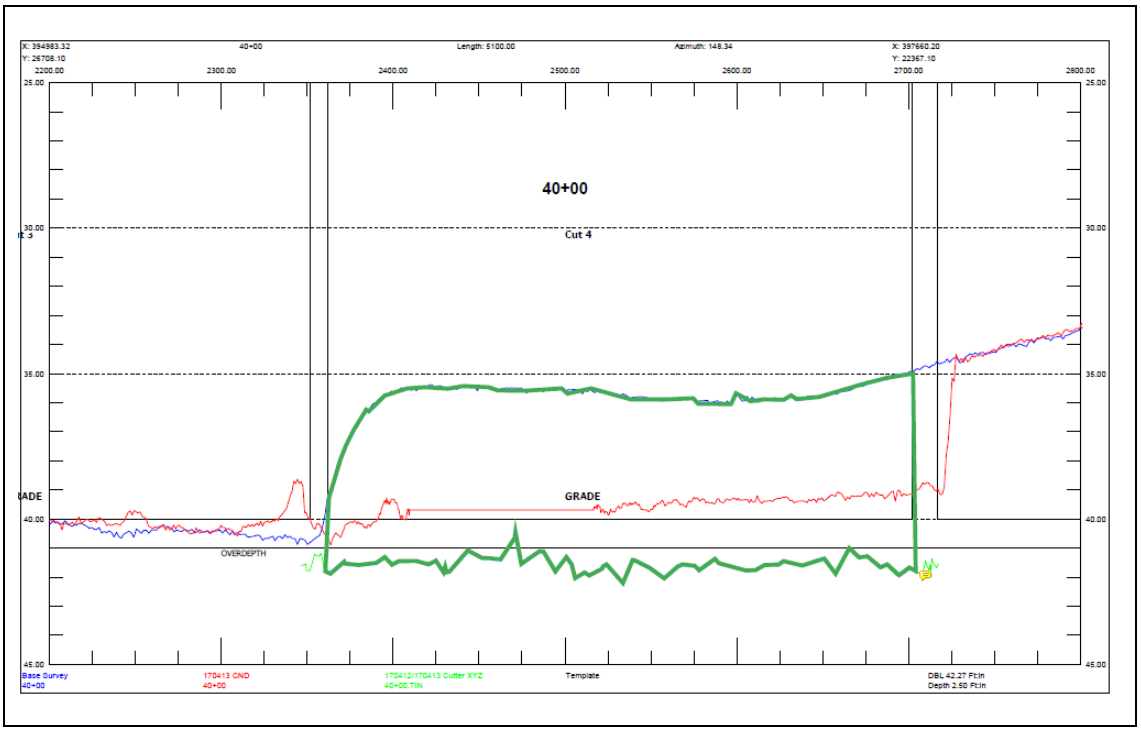

Figure 23: Hydrographic survey showing the contour (green) of the cutting production at 40+00.

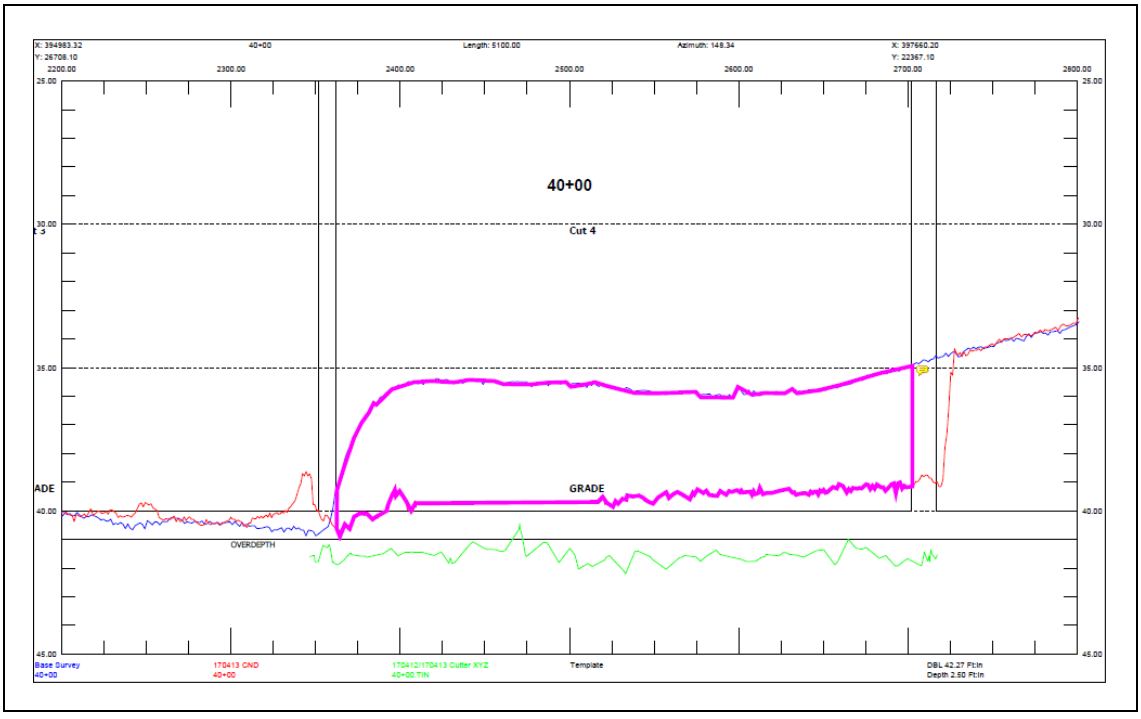

Figure 24: Hydrographic survey showing the contour (pink) of the production obtained at 40+00.

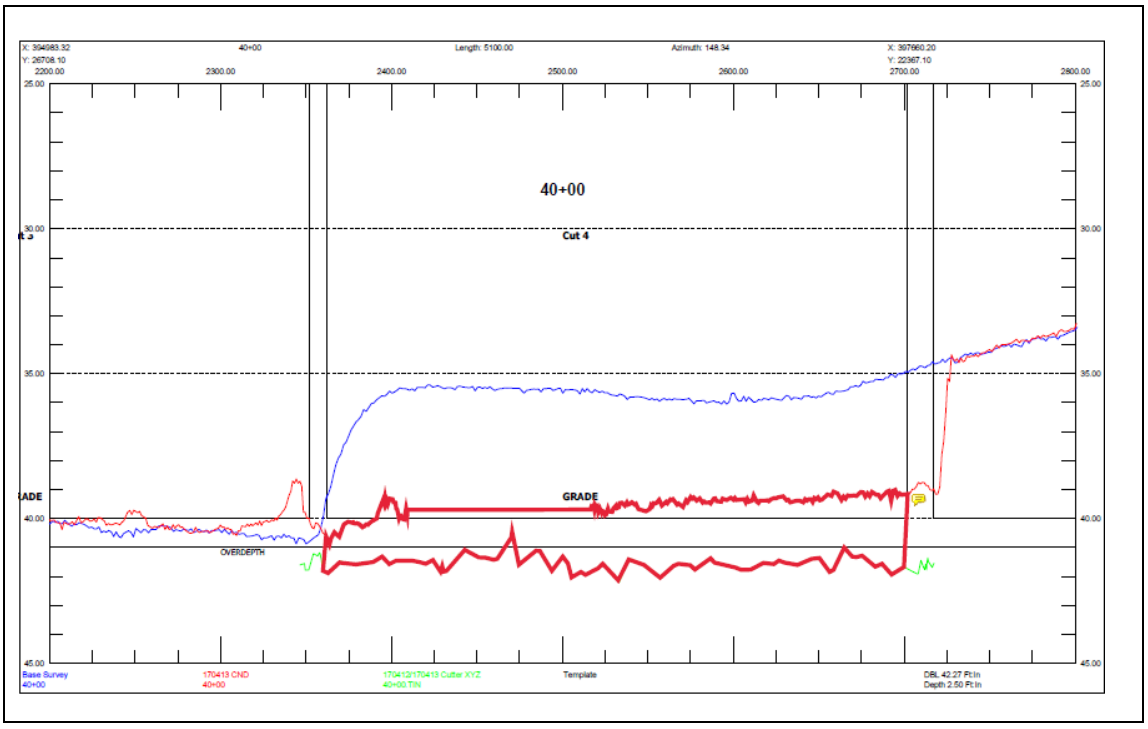

Figure 25: Hydrographic survey showing the contour (red) of spillage at 40+00.

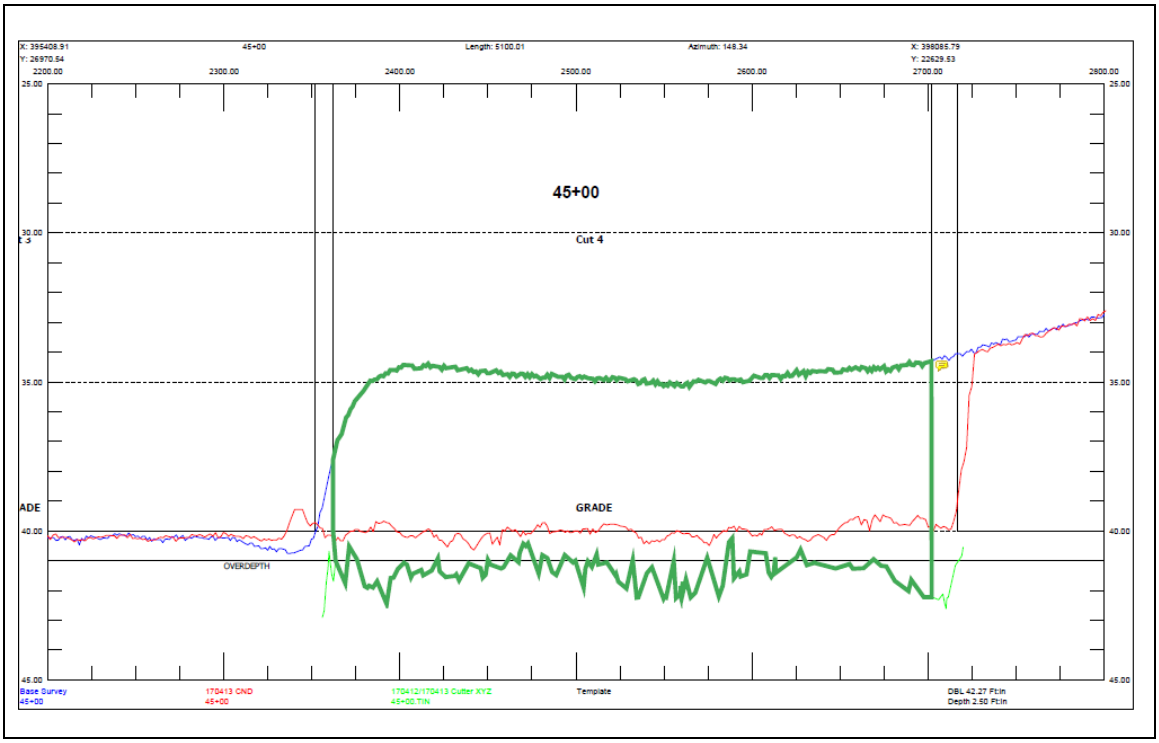

Figure 26: Hydrographic survey showing the contour (green) of the cutting production at 45+00.

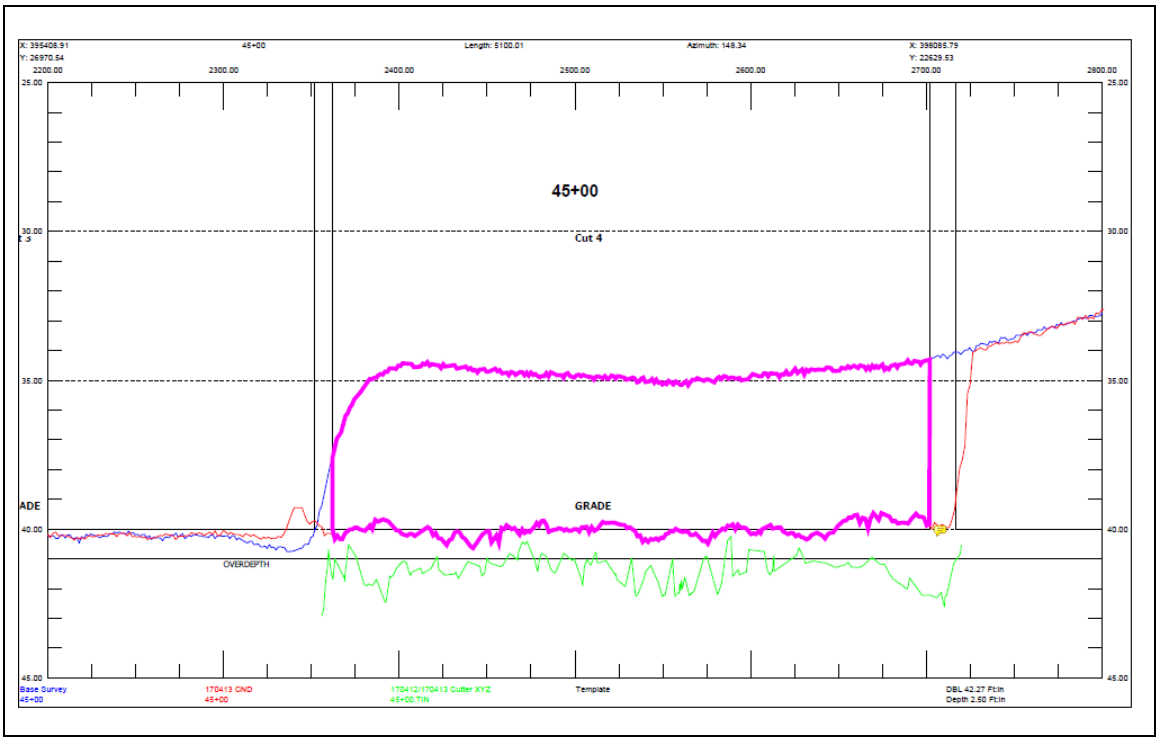

Figure 27: Hydrographic survey showing the contour (pink) of the production obtained at 45+00.

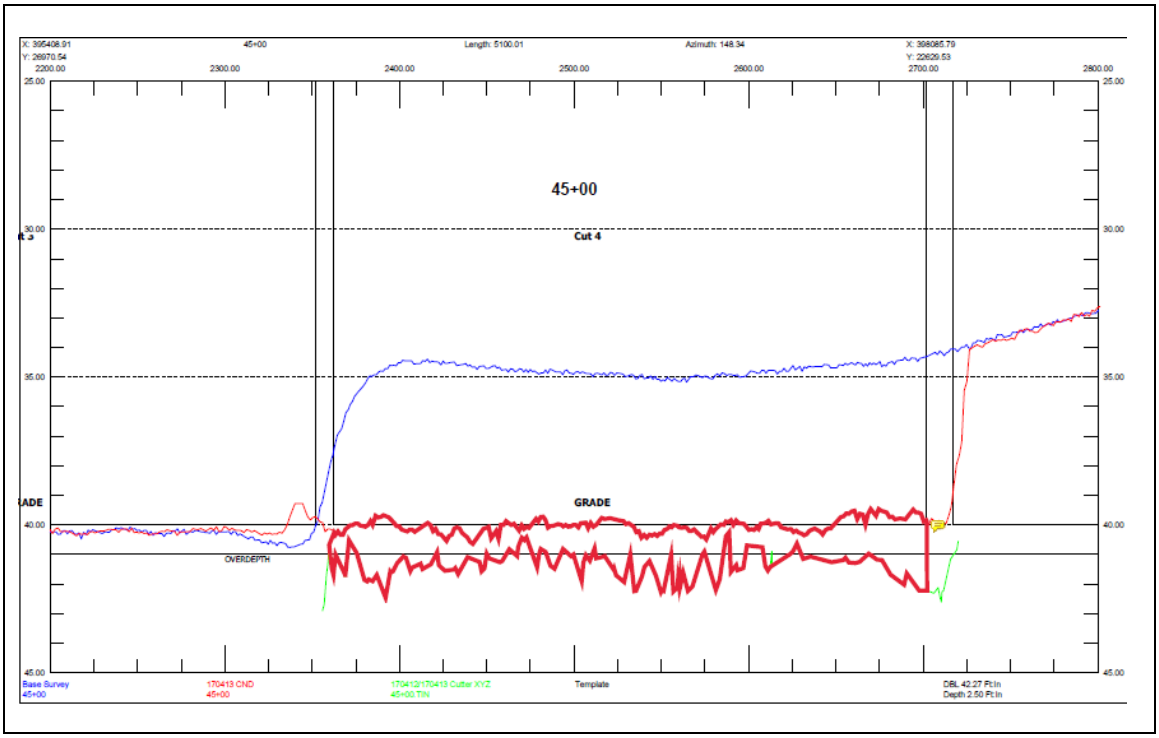

Figure 28: Hydrographic survey showing the contour (red) of spillage at 45+00.

Figure 26 shows the hydrographic survey that is obtained from location '45+00' of 'Cut 4'. The contour highlighted shows the cutting production and if this contour is measured, an area of about 21.01 m^2 is obtained. Similarly, the production is shown by the contour in Figure 27 and measures about an area of 16.75 m^2. Using these two areas, the area of the spillage contour can be obtained, i.e. spillage = cutting production – actual production which gives an area 4.26 m^2. Now the percentage of spillage is basically the ratio of the amount of spillage to the cutting production, i.e. spillage (%) = spillage/cutting production which gives a value of 20.3%.

Hydrographic surveys from location '41+00' of 'Cut 4' estimates spillage at 34% whereas at location '42+00', spillage is 23.2%. At location '43+00' and '44+00', spillage is at 32.9% and 29.9% respectively (see Appendix B). The spillage values obtained is scattered because while dredging at certain locations, The Texas had choking issues with the pump. Also, the cutter head of The Texas employs a screen to block out ordinances. Although, the material dredged is sand, there were shells present in the seabed and these shells got stuck in the screen thus reducing production.

Therefore, the range for spillage can be assumed to be 20%-34%. The model provides a spillage of ~38% and when compared with real-life data, it can be stated that the spillage obtained from the model is in close proximation with the values obtained in the industry. Hence, the model is valid and provides an approximate value for spillage.

6.3 Comparison with experimental results.

In order to further validate the model, the results obtained from the model are compared with the results obtained from the experiments performed by Burger (2003). As mentioned in Chapter 3, Burger performed actual cutting tests in cemented banks of gravel in order to determine production and spillage as a function of the operational parameters. A number of mixture velocities were used in the experiments and the production percentage were found for each of the mixture velocities used and these data are plotted and compared.

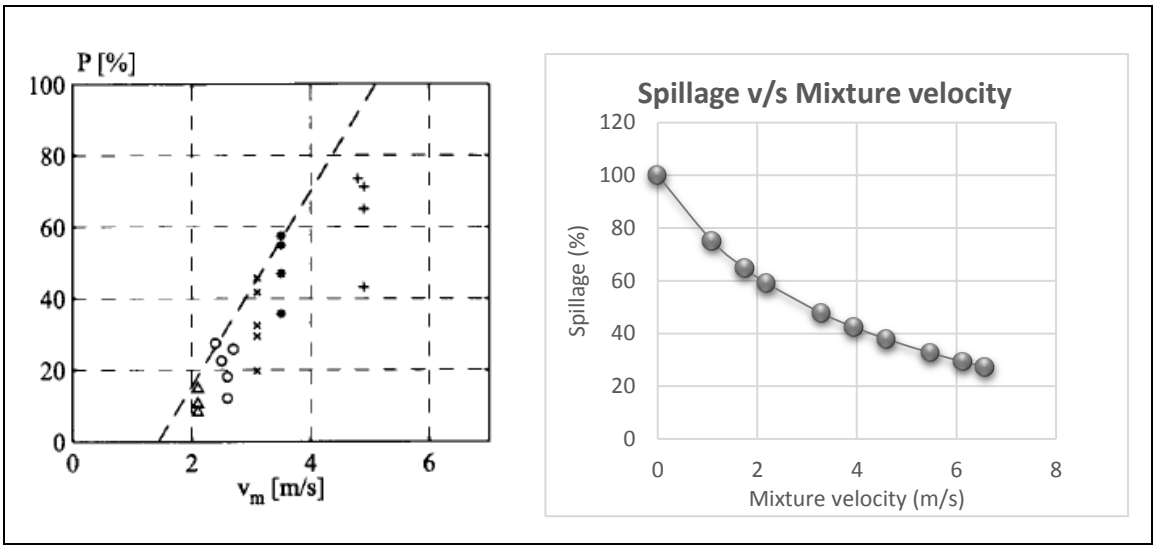

Figure 29: Comparison of mixture velocity between experimental results (left) and model results (right).

Figure 29 shows the comparison between the graph plotted from the experiments performed by Burger (2003) on the left and the graph obtained from the model on the right. In the plot on the left, the production percentage is plotted against the mixture velocity for the different rotational velocities. The plot shows that the maximum production percentage varies almost linearly with the mixture velocity. In the plot on the right, the spillage is plotted against the mixture velocity. The plot shows that spillage varies almost linearly with the mixture velocity disregarding the data point at v_m=0.

The linear increase in production implies that spillage decreases linearly. This is true because the total cutting production is the sum of production and spillage. Increasing the mixture velocity implies that the suction flow within the cutter head is increased. Increasing the suction flow, increases the region of influence of the suction mouth and therefore more particles can be entrained into the suction mouth thereby increasing production. If the production increases, this means that spillage will correspondingly decrease which is exactly what the graphs predict. Hence, it can be said that the model behaves in a similar fashion when compared to the experiments performed.

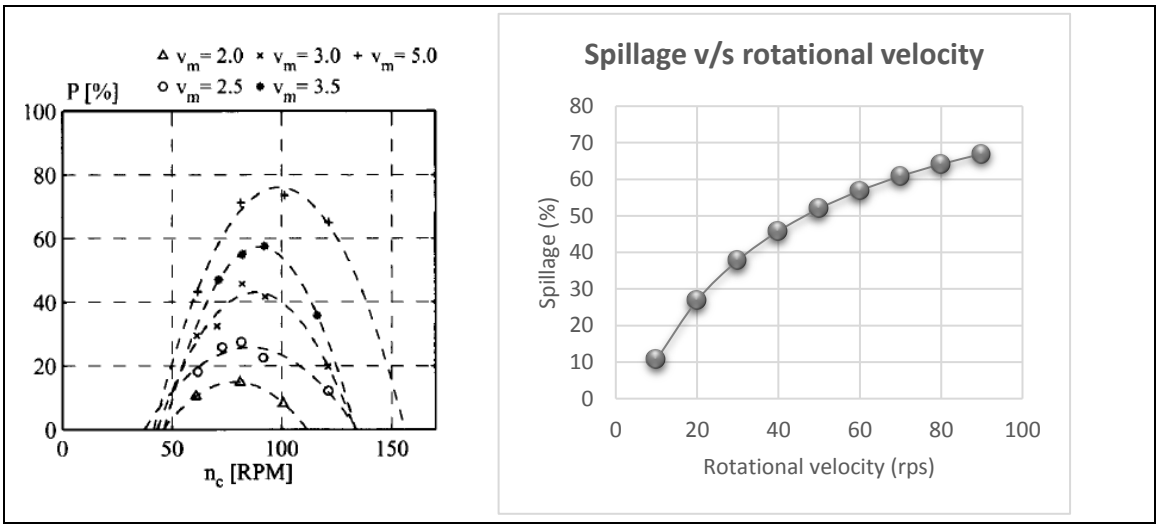

Figure 30: Comparison of rotational velocity between experimental results (left) and model results (right).

Furthermore, the results regarding the rotational velocity is also compared. Figure 30 shows the comparison between the graph plotted from the experiments plotted by Burger (2003) on the left and the graph obtained from the model on the right. In the plot on the left, the production percentage is plotted against the rotational velocity for different mixture velocities. The plot shows that initially the production percentage increases with an increase in rotational velocity but after a certain optimum is reached, any further increase in rotational velocity results in a decrease in production percentage. The most likely reasons for the increase in production percentage with increasing rotational velocity are better mixing of the particles due to collisions of particles with the blades and positive change of flow within the cutter head (Burger 2003).

In the plot on the right, spillage is plotted against the rotational velocity. The plot shows that spillage increases with an increase in rotational velocity. When the two plots are compared, it can be seen that at low rotational velocities both production and spillage is low. The reason for this is because a low rotational velocity results in a low cutting production and therefore both production and spillage is at a minimum. When the rotational velocity is increased, the cutting production also increases as more material is cut from the seabed thereby increasing both production and spillage with the increase of production being greater than that of spillage. This explains why the production percentage increases in the initial phase of the left plot. After the optimum has been reached, the increase in production and spillage is reversed with spillage being greater

than that of production and that explains the downward slope in the second phase of the left plot which is also justified in the results obtained from the model.

6.4 Summary.

Since experiments are unable to be conducted, the hydrographic surveys obtained from The Texas are used to validate the model. Contours are drawn on the surveys and the total cutting production area along with the actual production area is measured. The difference between these two areas results in the area of spillage and the spillage percentage is calculated as the ratio of spillage area to total cutting production area. The range of spillage obtained from the surveys is about 20-34% and the model gives a spillage of 38%. Hence, it can be stated that the spillage obtained from the model is in close proximation with the values obtained in the industry.

In order to further validate the model, the results obtained from the model are compared with the results obtained from experiments performed by Burger (2003). Burger found a relationship between the production percentage and the mixture velocity and stated that the production percentage varies almost linearly with the mixture velocity. A similar trend is observed in the model when the spillage is compared to the mixture velocity. Also, Burger compared the production percentage with the rotational velocity and found that an initial increase in rotational velocity increases production but after a certain optimum is reached, any further increase in rotational velocity causes a decrease in production. Similarly, in the model, spillage is compared with the rotational velocity and it is observed that an increase in rotational velocity causes the spillage to increase as well. Thus, the model behaves in a similar fashion as that of the results from the experiments conducted by Burger (2003). Also, since the model provides a spillage value that is relatable to the industry, it can be concluded that the model, although simple, is able to provide a realistic value for spillage and is therefore validated.

7

Conclusions & Recommendations

7.1 Conclusions.

The activities described in this thesis are part of a general effort to develop an accurate and efficient numerical model to estimate spillage. The current thesis focuses only on Type-2 spillage since this is the first model created and will be used as a foundation for a more complex and accurate model. The results obtained from the model are studied and the conclusions reached are elaborated below.

General remarks

As seen in the previous chapter, the influence of the suction flow, rotational velocity of the cutter and the swing speed of the cutter on spillage is in line with what is observed in practice. The model assumes that the particles cut will follow the flow of fluid without any deviation in its path thus implying that particle size is not taken into account. For higher particle size, the particles will deviate from the flow path of the fluid since inertia will play an important role.

Also, the value of spillage obtained (~38%) is close to the values obtained in the dredging industry. In practice, the range of spillage is between 20 – 34% and in comparison, the value of spillage obtained from the model is in close proximity. So, the model, although simple, is working as intended.

7.2 Recommendations for future research.

The current model uses a simplistic approach to obtain spillage and can definitely be improved upon in order to make it more accurate and efficient. In order to make this possible, more variables need to be taken into account and experiments need to be conducted in order to further validate the model. The following points refer to improvements and additional tasks that can be done in order to improve the current model.

- Internal volume of the cutter:

  The current model does not take into account the internal structure of the cutter head. The presence of the shaft plays a contributing factor to flow within the cutter due to friction losses along the shaft. Moreover, if the cutter head employs a conical back plate and a screen (to keep out ordinances) as shown in Figure 2 then the effective internal volume of the cutter head will be reduced which will affect the flow out of the cutter and in turn spillage.

- Particle – particle interaction:

  The particles that enter the cutter head are assumed to follow the flow path of the fluid thus ignoring particle – particle interaction, which will be a major factor that determines the flow field within the cutter head. The particle – particle interaction would also affect the particle trajectories eventually affecting spillage.

- Cutter head geometry:

  The current model assumes the cutter head to be a truncated cone. By doing this, an accurate flow cannot be calculated since the cutter geometry is an essential component. Thus, by taking into consideration the geometry of the cutter head, an accurate value for spillage can be obtained.

- Particle shape/size:

  The shape of particles varies and is not uniform. Not all particles will be spherical in shape. As mentioned before, the size of particles is crucial to determine whether the particles follow the flow path of the fluid or deviate from it.

- Flow field within the cutter:

  The mixing process within the cutter is a complex process and thus dedicated software need to be used to solve this issue. Since the current model is a simple one it only uses a spreadsheet to estimate spillage. A preferable option would be to use a CFD package to determine the flow field within the cutter which could then predict the trajectories of the particles within the cutter.

Bibliography

Bluemink, J.J., Lohse, D., Prosperetti, A., Van Wijngaarden, L. (2009). “Drag and lift forces on particles in a rotating flow.” Journal of Fluid Mechanics, Cambridge University Press 2009, pp. 1-31.

Burger, M. den. (2003). “Mixture Forming Processes in Dredge Cutter Heads.” Ph.D. Dissertation, Delft University of Technology, The Netherlands.

Burger M. den, and Talmon A. M. (2002), "Particle trajectories along a cutter head blade, using the results of a CFD model for the flow”, proc. Dredging ‘02 Key Technologies for Global Prosperity, Orlando, USA, pp. 1-13.

Burger, M. den, Vlasblom, W.J., and Talmon, A.M. (1999), "Influence of Operational Parameters on Dredge Cutterhead Spillage", proc. CEDA Dredging Days 1999, Amsterdam, The Netherlands.

Dekker, M. A., den Burger, M., Kruyt, N. P., and Vlasblom, W. J. (2003). “Experimental and Numerical Investigation of Cutter Head Dredging Flows.” Journal of Waterway, Port, Coastal and Ocean Engineering, ASCE, Vol. 129, No. 5, pp. 203-209.

Dismuke, C. P. (2012). “Experimental Investigation of the Flow Field in the Vicinity of the Suction Inlet of a Model Cutter Suction Dredge.” Master Thesis, Texas A&M University, USA.

Henriksen, J. C. (2009). “Near-Field Sediment Resuspension Measurement and Modeling for Cutter Suction Dredging Operations. Ph.D. Dissertation, Texas A&M University, USA.

Hofstra, C. F., Miedema, S. A. and van Rhee, C. (2010). “Particle Trajectories near Impeller Blades in Centrifugal Dredge Pumps.” WODCON XIX, Beijing China, September 2010.

Karassik, I. J., Messina, J. P., Cooper, P., and Heald, C. C., (2001). “Pump Handbook.” Third Edition, McGraw-Hill, ch-2.

Manikantan, A. K. (2009). “Comparing Methods for Measuring the Volume of Sand Excavated by a Laboratory Cutter Suction Dredge Using an Instrumented Hopper Barge and a Laser Profiler.” Master Thesis, Texas A&M University, USA.

Miedema, S. A., Personal communication. April 2017.

Nieuwboer, B. J., Keetels, G. H., van Rhee, C. (2017). “Flow velocities in an axi-symmetrical rotating cutter suction head.” 18th Transport and Sedimentation Conference.

Tagawa, Y., Van der Molen, J., Van Wijngaarden, L., Sun, C. (2012). “Wall forces on a sphere in a rotating liquid-filled cylinder.” Physics of Fluid Group, Faculty of Science and Technology, J. M. Burgers Centre for Fluid Dynamics, University of Twente, The Netherlands.

Talmon, A. M., Vlasblom, W. J. and Burger, M. den. “Cutter Production and Kinematics of Mixture Forming.” 19th World Dredging Congress, ch-20.

van Rhee, C., Bezuijen, A. (1998). “The Breaching of Sand Investigated in Large-Scale Model Tests.” Coastal Engineering.

van Rhee, C. (2015). “Slope Failure by Unstable Breaching.” Proceedings of the Institution of Civil Engineers, Maritime Engineering 168 June 2015 Issue MA2, pp. 84-92.

Wilson, K.C., Addie, G.R., Sellgren, A. and Cliff, R. “Slurry Transport using centrifugal pumps”, third edition.

Xu, Y., Xu, C., Zhou, Z., Du, J., Hu, D. (2009). “2D DEM simulation of particle mixing in rotating drum: a parametric study.” College of Science, China Agricultural University, Beijing, China.

A

Hydrographic Surveys

Figure 31 shows the hydrographic survey that is obtained from location '41+00' of 'Cut 4'. The contour highlighted shows the cutting production and if this contour is measured, an area of about 19.98 m^2 is obtained. Similarly, the production is shown by the contour in Figure 32 and measures about an area of 13.19 m^2. Using these two areas, the area of the spillage contour can be obtained, i.e. spillage = cutting production – actual production which gives an area 6.79 m^2. Now the percentage of spillage is basically the ratio of the amount of spillage to the cutting production, i.e. spillage (%) = spillage/cutting production which gives a value of 34%.

Figure 33 shows the hydrographic survey that is obtained from location '42+00' of 'Cut 4'. The contour highlighted shows the cutting production and if this contour is measured, an area of about 20.38 m^2 is obtained. Similarly, the production is shown by the contour in Figure 34 and measures about an area of 15.65 m^2. Using these two areas, the area of the spillage contour can be obtained, i.e. spillage = cutting production – actual production which gives an area 4.73 m^2. Now the percentage of spillage is basically the ratio of the amount of spillage to the cutting production, i.e. spillage (%) = spillage/cutting production which gives a value of 23.2%.

Figure 35 shows the hydrographic survey that is obtained from location '43+00' of 'Cut 4'. The contour highlighted shows the cutting production and if this contour is measured, an area of about 22.50 m^2 is obtained. Similarly, the production is shown by the contour in Figure 36 and measures about an area of 15.09 m^2. Using these two areas, the area of the spillage contour can be obtained, i.e. spillage = cutting production – actual production which gives an area 7.41 m^2. Now the percentage of spillage is basically the ratio of the amount of spillage to the cutting production, i.e. spillage (%) = spillage/cutting production which gives a value of 32.9%.

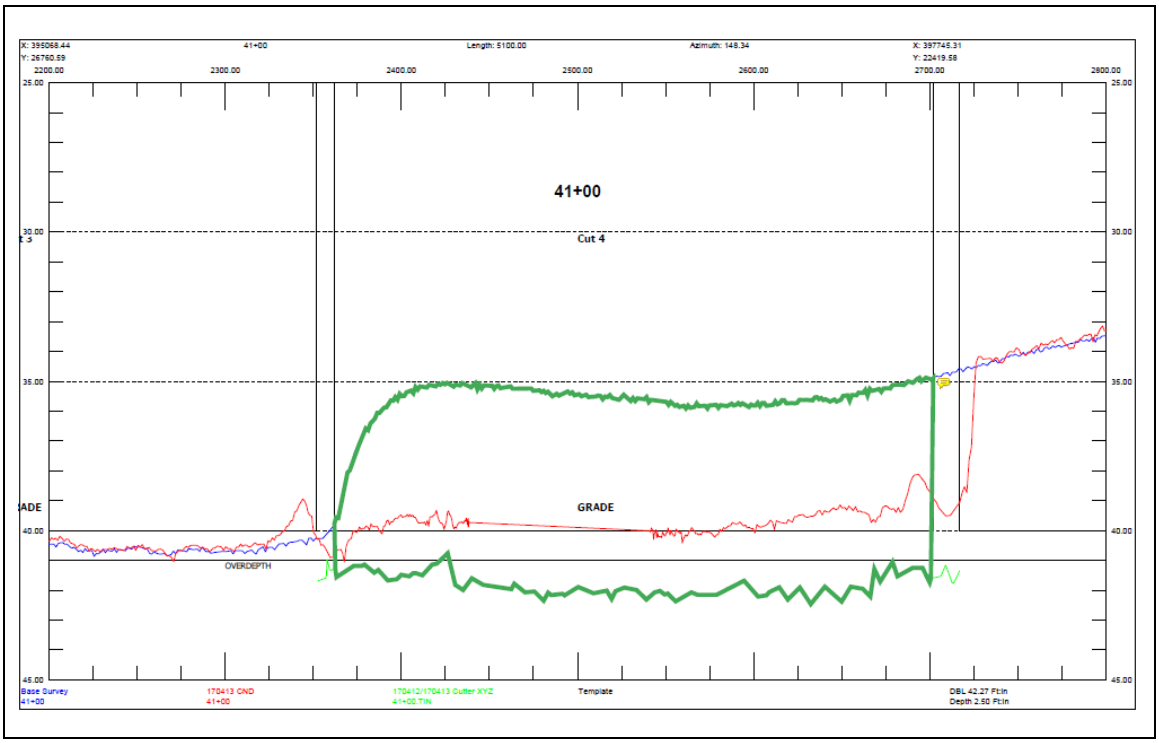

Figure 31: Hydrographic survey showing the contour (green) of the cutting production at 41+00.

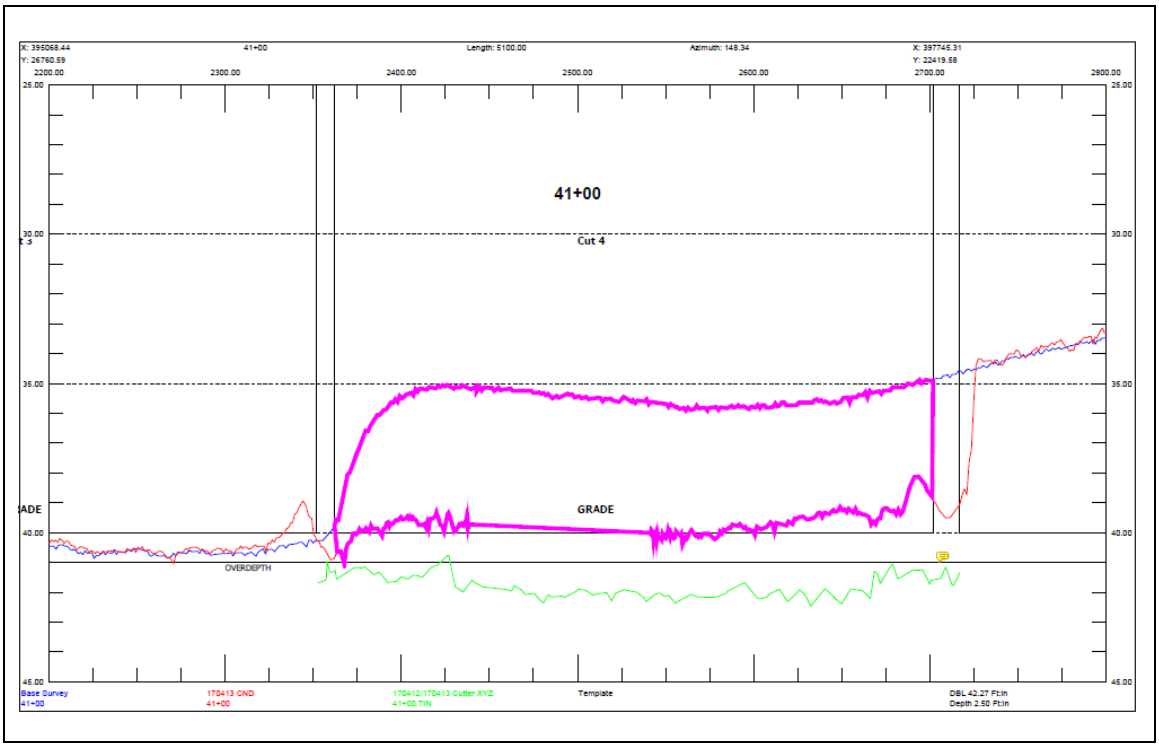

Figure 32: Hydrographic survey showing the contour (pink) of the production obtained at 41+00.

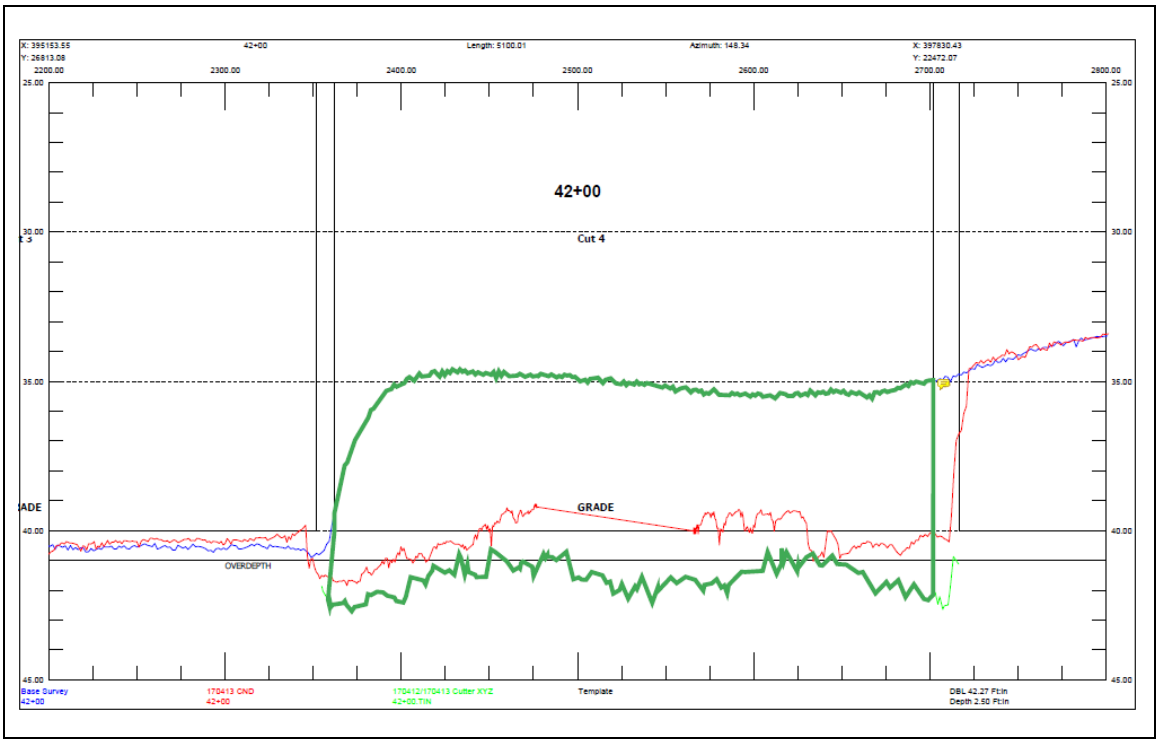

Figure 33: Hydrographic survey showing the contour (green) of the cutting production at 42+00.

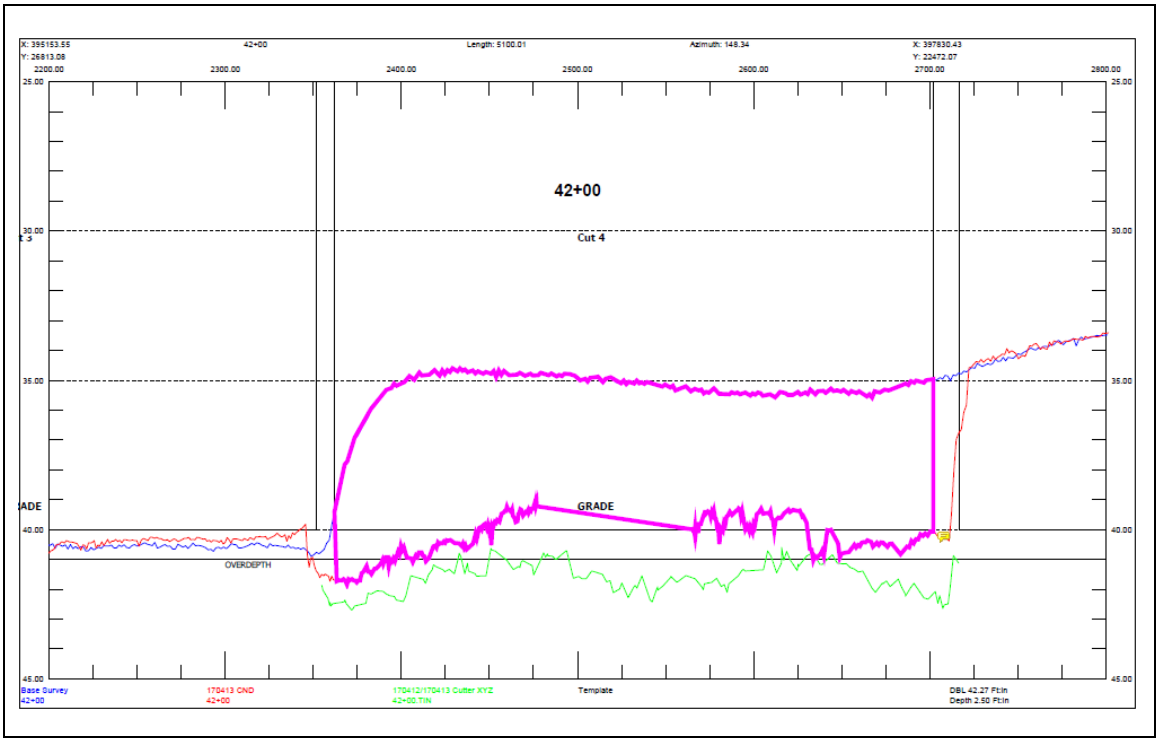

Figure 34: Hydrographic survey showing the contour (pink) of the production obtained at 42+00.

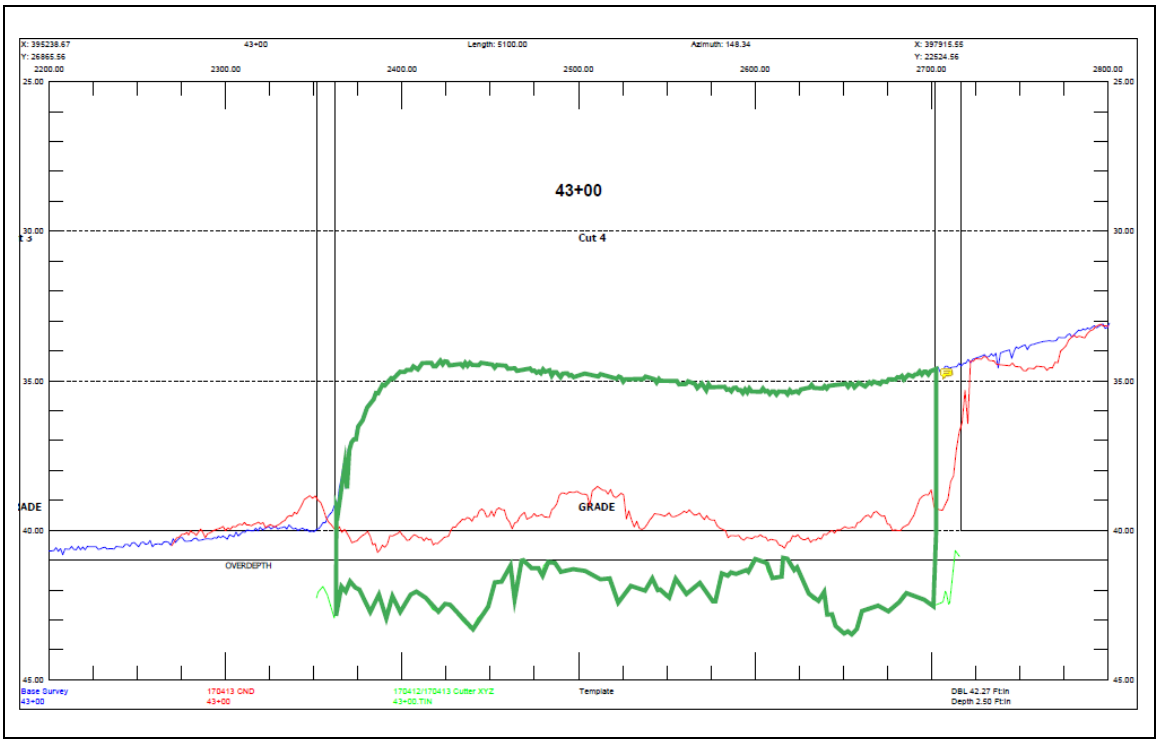

Figure 35: Hydrographic survey showing the contour (green) of the cutting production at 43+00.

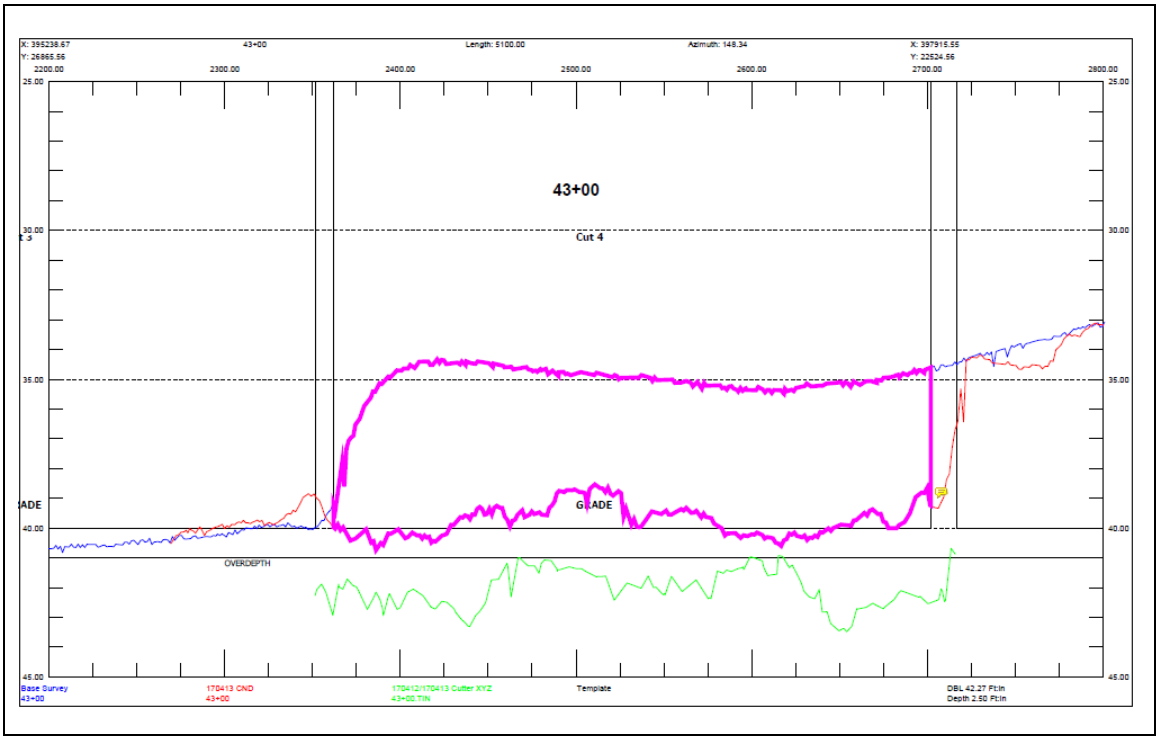

Figure 36: Hydrographic survey showing the contour (pink) of the production obtained at 43+00.

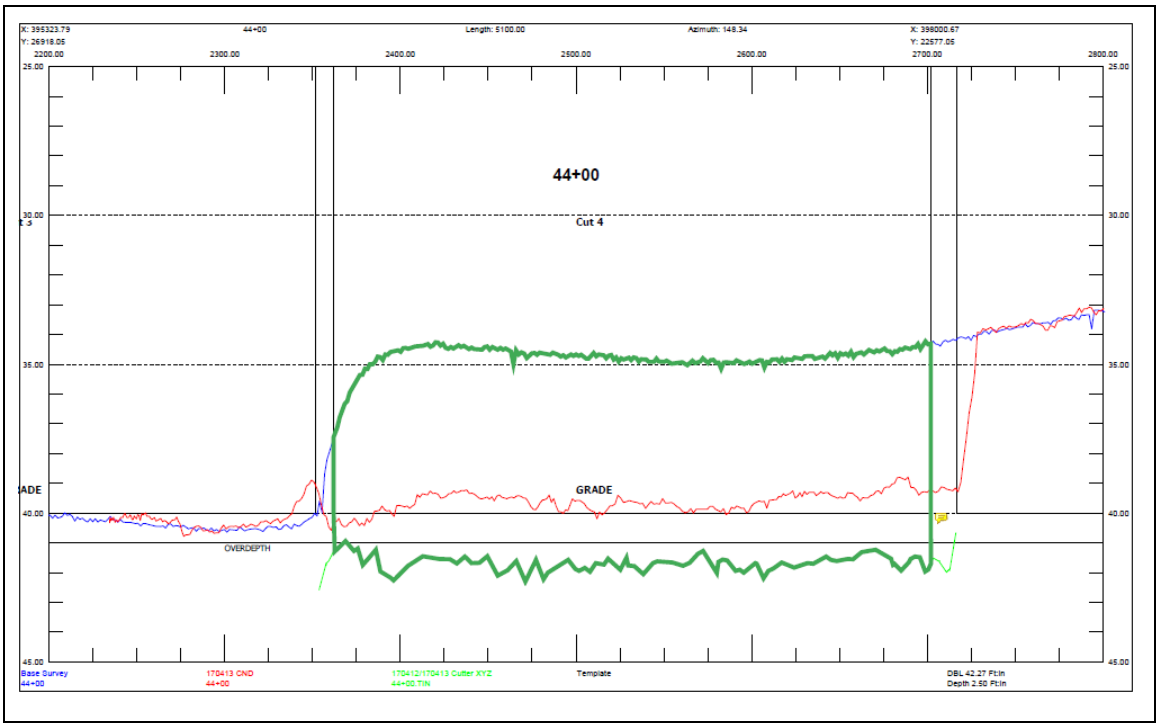

Figure 37: Hydrographic survey showing the contour (green) of the cutting production at 44+00.

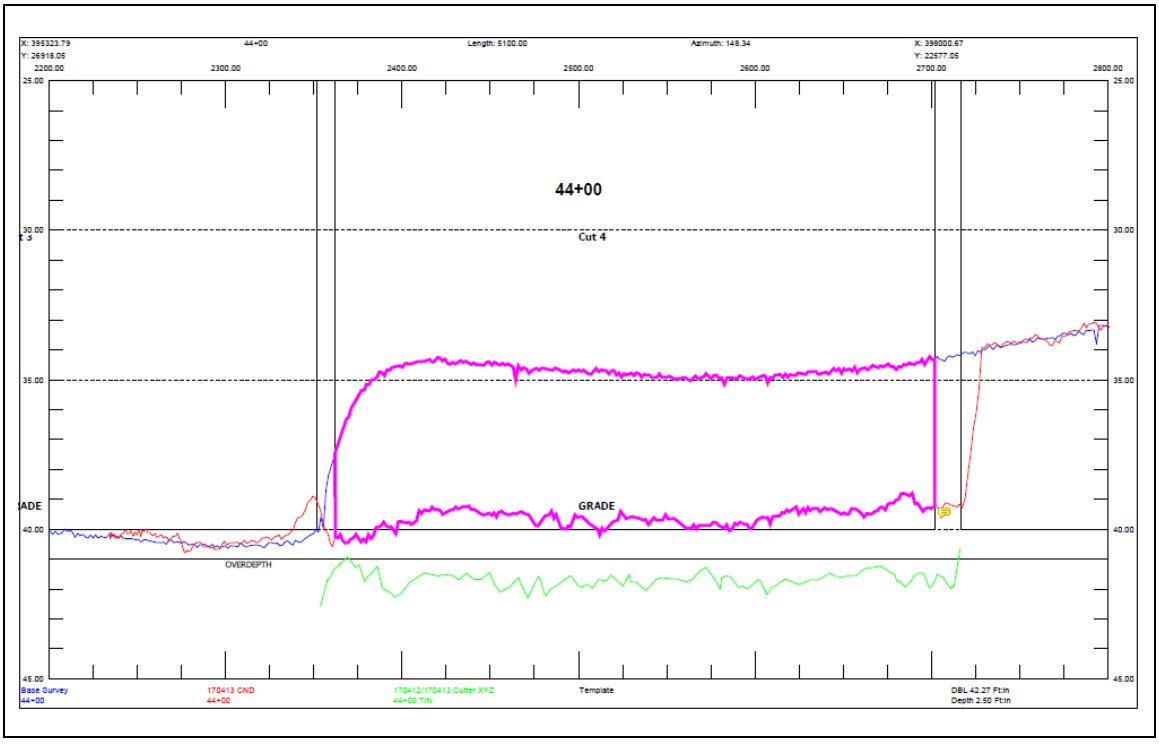

Figure 38: Hydrographic survey showing the contour (pink) of the production obtained at 44+00.

Figure 37 shows the hydrographic survey that is obtained from location '44+00' of 'Cut 4'. The contour highlighted shows the cutting production and if this contour is measured, an area of about 22.28 m^2 is obtained. Similarly, the production is shown by the contour in Figure 38 and measures about an area of 15.62 m^2. Using these two areas, the area of the spillage contour can be obtained, i.e. spillage = cutting production – actual production which gives an area 6.66 m^2. Now the percentage of spillage is basically the ratio of the amount of spillage to the cutting production, i.e. spillage (%) = spillage/cutting production which gives a value of 29.9%.

B

Base Model

The base model proposed by Miedema (2017) is based on the pump affinity laws. It assumes that there is an inflow close to the nose of the cutter head and an outflow near the cutter ring. Since a distinct separation between the region of inflow and outflow is hard to predict, the cutter head is assumed to be divided into 2 slices with the top slice having an inflow and the bottom slice having an outflow. Equations of flow and pressure are derived from the affinity laws. The equations for pressure and flow for the flow without mixture are derived as follows:

(1)

General

$$p = \alpha n^2 D_4^2$$
$$Q = \beta n D^2 w$$

Specific flow

$$q = \frac{Q}{w} = \beta n D^2 = \frac{\beta}{\alpha n} p$$

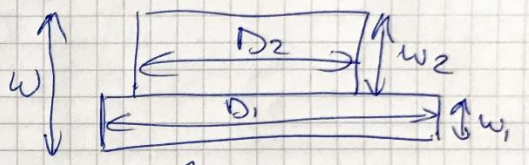

So:

$$p_1 = \alpha n^2 D_1^2$$
$$Q_1 = \beta n D_1^2 w_1$$
$$q_1 = \frac{\beta}{\alpha n} p_1$$

$$Q_2 = (q_2 - q_1) w_2 = \left(\frac{\beta}{\alpha n} p_2 - \frac{\beta}{\alpha n} p_1\right) w_2$$
$$Q_2 = \frac{\beta}{\alpha n} (p_2 - p_1) w_2 \qquad Q_1 = \frac{\beta}{\alpha n} p_1 w_1$$

Flow is circulating so:

$$Q_1 + Q_2 = 0$$
$$\frac{\beta}{\alpha n} p_1 w_1 + \frac{\beta}{\alpha n} (p_2 - p_1) w_2 = 0$$
$$\frac{\beta}{\alpha n} \left(p_1 w_1 + (p_2 - p_1) w_2\right) = 0$$
$$\Rightarrow p_1 w_1 + (p_2 - p_1) w_2 = 0$$
$$\Rightarrow \frac{w_1}{w_2} = \frac{p_1 - p_2}{p_1} = \frac{\alpha n^2 (D_1^2 - D_2^2)}{\alpha n^2 D_1^2}$$
$$\Rightarrow \frac{w_1}{w_2} = \frac{D_1^2 - D_2^2}{D_1^2} = \frac{w_1}{w - w_1}$$

(2)

$$w_1 = (w - w_1) \cdot \frac{D_1^2 - D_2^2}{D_1^2}$$

With: $$f = \frac{D_1^2 - D_2^2}{D_1^2}$$

$$w_1 = w \frac{f}{1+f}$$

Circulating flow is now:

$$Q_c = Q_1 = 3 n D_1^2 w \frac{f}{1+f}$$

This is without mixture flow

With mixture flow: (3)

positive = leaving the cutter.

$$Q_1 + Q_m + Q_2 = 0$$

(Q_1: positive, Q_m: positive, Q_2: negative)

$$\frac{\beta}{\alpha_h} p_1 \omega_1 + Q_m + \frac{\beta}{\alpha_h}(p_2 - p_1)\omega_2 = 0$$

$$\frac{\beta}{\alpha_h}\left(p_1 \omega_1 + (p_2 - p_1)\omega_2\right) + Q_m = 0$$

$$p_1 \omega_1 + (p_2 - p_1)\omega_2 + \frac{\alpha_h}{\beta} Q_m = 0$$

$$p_1 \omega_1 + (p_2 - p_1)(\omega - \omega_1) + \frac{\alpha_h}{\beta} Q_m = 0$$

$$p_1 \omega_1 = (p_1 - p_2)\omega_2 - \frac{\alpha_h}{\beta} Q_m$$

$$\omega_1 = \frac{(p_1 - p_2)}{p_1}\omega_2 - \frac{\alpha_h}{\beta}\frac{Q_m}{p_1}$$

With: $p_1 = \alpha_h^2 D_1^2$ $\quad p_2 = \alpha_h^2 D_2^2$.

$$\omega_1 = \frac{(D_1^2 - D_2^2)}{D_1^2}\omega_2 - \frac{\alpha_h}{\beta}\frac{Q_m}{\alpha_h^2 D_2^2}$$

$$\omega_1 = \frac{(D_1^2 - D_2^2)}{D_1^2}\omega_2 - \frac{1}{\beta_h}\frac{Q_m}{D_2^2}$$

$$\omega_1 + \omega_1 f = \omega f - \frac{1}{\beta_h}\frac{Q_m}{D_2^2}$$

$$\omega_1 = \frac{\left(\omega f - \frac{1}{\beta_h}\frac{Q_m}{D_2^2}\right)}{1 + f}$$

$$\omega_2 = \omega - \omega_1$$

(4)

The circulating flow is now:

$$Q_c = Q_1 = \beta_n D_1^2 w_1$$

The total flow through the cutter is:

$$Q_t = Q_c + Q_m$$

$$Spillage = \frac{Q_c}{Q_c + Q_m}$$

Model is based on particles following the flow. Particles leaving the cutter with Q_1 will not come back into the cutter.

I used $\beta = 0.02$ which is just a first guess.

The model can be optimized in many ways. So just see it as a start.